Deltares

Effect of offshore wind farms on waves and currents

Offshore Wind Energy Shipping Safety Monitoring and Research Programme (MOSWOZ)

Effect of offshore wind farms on waves and currents
Offshore Wind Energy Shipping Safety Monitoring and Research Programme (MOSWOZ)

Author(s)
Caroline Gautier
Antonios Emmanouil
Leo Leummens

Effect of offshore wind farms on waves and currents
Offshore Wind Energy Shipping Safety Monitoring and Research Programme (MOSWOZ)

Client	Rijkswaterstaat Zee en Delta
Contact	Vivian Baetens
Projectreference	SITO-PS INF15-Scheepvaartveiligheid rondom windparken
Keywords	Offshore wind farms, North Sea, shipping safety, MOSWOZ

Document control	
Version	1.0
Date	12-12-2025
Project nr.	11211512-002
Document ID	11211512-002-HYE-0001
Pages	64
Classification	
Status	Final

Author(s)		
	Caroline Gautier Antonios Emmanouil Leo Leummens	

The allowed use of this table is limited to check the correct order-performance by Deltares. Any other client-internal-use and any external distribution is not allowed.

Doc. version	Author	Reviewer	Approver
1.0	Caroline Gautier Antonios Emmanouil Leo Leummens	Sofia Caires	Paul van Steeg

Summary

This report, prepared under the MOSWOZ (Offshore Wind Energy Shipping Safety Monitoring and Research Programme), investigates the effects of offshore wind farms (OWFs) on waves, currents, and water levels in the North Sea, with implications for shipping safety.

The North Sea hosts intensive shipping traffic and expanding OWF infrastructure. The study aims to assess whether OWFs significantly affect hydrodynamic and wave conditions, identify dependencies, and evaluate potential risks for navigation.

The objectives of the study are twofold:

1. the development of a semi-advanced model to incorporate the OWF effects on the surface winds;
2. the analysis of the dependency on meteorological and physical conditions of the OWF effects on the current and wave conditions.

The introduced method to generate synthetic wind fields using ERA5 data, incorporating wake effects and condition-dependent wind deficits improves realism compared to previous uniform 10% wind speed reduction approach and enables more accurate long-term simulations beyond the one-year of the accurate WINS50 dataset.

In terms of effects, OWFs generally lead to minor changes in current velocity, with instantaneous differences up to 0.5 m/s inside wind farms. There are no strong relations between the effects on the current and the wind speed, direction, or atmospheric stability; proximity to OWFs is the dominant factor. The largest impacts occur within OWFs, potentially relevant for small vessels navigating inside wind parks.

The OWFs when operating, typically lead to a reduction of significant wave height (Hs) by ~4% across OWFs and surrounding navigational areas. This reduction is consistent across wind speed classes and most atmospheric conditions (unstable and neutral). Under stable atmospheric conditions (rare, ~5% occurrence), wave reduction is negligible; whereas slight amplification may occur in energetic wave conditions.

Overall, OWF-induced changes in currents and waves are generally modest and unlikely to pose immediate hazards for large-scale navigation. Localized effects within OWFs and wake zones warrant attention for small craft and operational planning.

Contents

1 Introduction

1.1 General

The North Sea is one of the busiest areas for shipping in the world. The effects of existing offshore wind farms (OWF) and the ambitious plans for additional wind farms and hub islands must be taken into account to ensure shipping safety. Therefore, Rijkswaterstaat has set up the Offshore Wind Energy Shipping Safety Monitoring and Research Programme (MOSWOZ). This programme studies the effect of offshore wind farms on shipping safety so that – if needed - measures can be taken to maintain levels of shipping safety.

One of the MOSWOZ topics is Hydro/Meteo. Within this topic the present study presents the effects of offshore wind farms on North Sea waves, currents and water levels, based on the results of existing numerical models.

In Deltares (2025) first steps were taken and a literature study was done on the subject. Two of the recommendations of that report are studied in the present follow up report:

- Semi advanced approach to account for the OWF effects on the wind — To overcome the limitation of having only one year of wind fields with the effect of the wind farms (including wake) fully modelled available we try to assess a parametric (semi-advanced) approach to include the effects of the OWF (including wake) on the wind fields by means of post-processing and derive long term wind fields.
- Dependencies — If we know where the effects that OWF's have on waves and currents depend on, we can make better warnings or assess the relevance of the effects.

The main goal of the Hydro/Meteo research is to help identifying if risk areas exist for shipping, due to the effects of the OWF on the waves and the currents, and whether mitigating measures are necessary. Currently, the wind farms are mainly optimized in terms of energy yield, within certain legislative constrains, mostly related to ecological and spatial planning aspects. Once the OWF effects on shipping safety have been identified, these can also be accounted for. The ultimate goal of the research being thus to contribute to a safer North Sea, helping consequently also with the prevention of environmental disasters due to shipping accidents.

1.2 Scope

The aim of this research is to determine to what extent offshore wind farms in the North Sea have an effect on waves and currents, and consequently on shipping safety. The focus of the present study is to find dependencies between the effects of OWF on currents and waves on the one hand and various variables like wind speed, wind direction, atmospheric stability on the other. Also, we make a start in the development of a quick semi-advanced method to compute the effect of OWFs on the wind fields.

1.3 Main message

No clear correlation could be found between the effects that offshore wind farms have on waves and currents on one hand and the wind speed, wind direction or atmospheric stability conditions leading to such effects on the other. There is a slight tendency that during stable atmosphere (warmer air above cold water), the effect of the OWF's on waves and currents is less than for neutral and unstable atmosphere.

1.4 Set up of the report

After this introducing Chapter 1, Chapter 2 describes how to derive semi advanced wind fields. The method for assessing dependencies is given in Chapter 3. In chapters 4 and 5 these dependencies are worked out for the flow velocities and wave conditions, respectively. Conclusions are given in Chapter 6.

2 Semi advanced approach for wind fields

2.1 Motivation

In the previous study, the hydrodynamic and wave numerical simulations with wind farm scenarios were carried out with:

i) The high resolution WINS50 wind fields, determined using a model that resolves the effects of wind farms on relevant atmospheric layers with high spatial accuracy and resolving the various time-dependent processes. Due to the computational expense of the advanced models computing the winds, these are available only for a very limited period (1 year) and for a certain area around the North Sea.

ii) Wind fields generated employing a relatively crude schematization of wind farm influence on the surface winds, namely a constant and spatially uniform wind speed reduction within the OWF's area. This wind speed reduction of 10% was applied to the ERA5 wind fields (Hersbach et al., 2020) which cover the whole globe and extend from 1979 onwards.

Ideally, to investigate the effects of OWF's on atmospheric, wave and current conditions within and around OWF's to assess nautical safety, it is necessary to simulate a longer duration than available in WINS50 wind fields (thus resolving for more-yearly extreme conditions that are most relevant). At the same time, a more accurate representation of the time-, condition-dependent and spatially varying processes evolving around an offshore wind farm is needed, than captured with the relatively crude schematization assuming a constant and uniform reduction of wind speeds only within the offshore wind farm polygons. A schematization that would also model the wake effects and a possible increase of wind speeds and hence of wave heights and current speeds around the windfarms in stable atmospheric conditions, should led to more realist results. It is noted that stable atmospheric conditions may occur less frequently but are most relevant for nautical safety around OWF's in the North Sea.

2.2 Methodology

A semi advanced approach has been developed to model efficiently the effects of operational wind farms on the surface wind speeds including wake effects as function of wind speed and direction, air temperature, water temperature, and the presence of OWF's. To that end, WINS wind fields are used to obtain the following characteristics of wakes from two relevant simulations, being the "WINS Control – No offshore wind farms" (WINS-CTL) and "WINS OWFs 2050" (WINS50):

- A condition dependent spatially-averaged wind deficit (or surplus) within the OWF polygon.
- A condition dependent wake length downwind from the OWF boundary, up to which a wind deficit above a certain threshold occurs.

Both characteristics are extracted as a function of wind direction, wind speed, atmospheric stability and area of the offshore wind farm. Aspects like lateral speed-up effects (evolving along either flank of wind wakes) are neglected at this stage as their importance is deemed secondary to the wind deficit in the context of the present study.

More in detail, all OWF's within the WINS50 domain are processed individually to extract the wind deficit and wake length. At each wind farm, and for each timestep within the available 1-year simulation of wind fields with the advanced WINS50, the predominant wind direction, wind speed magnitude and atmospheric stability condition are determined using the WINS50

control simulation by accounting for all grid points that fall within the OWF polygon. To achieve that, the following classes are considered:

- 3x classes for Atmospheric conditions: Unstable ($\Delta T < -1.5$ °C), Neutral ($1.5 < \Delta T < 1.5$ °C) and Stable ($\Delta T > 1.5$ °C) atmosphere, where $\Delta T = T_{2m}$ - SST. (SST = sea surface temperature);
- 5x classes for wind speed at 10m : 1.0-2.5, 2.5-6.5, 6.5-13, 13-20, >20 m/s, roughly representing the various turbine behaviour regimes: below cut-in, cut-in to efficient generation, rated power, beyond cut-out. At wind speeds below 1 m/s wake effects are minor, and thus not considered to avoid noise in the obtained statistics;
- 8x classes for wind direction at 10m: 45° sectors (0-45°N, …, 315-360°N), covering the full circle.

Overall, this yields a total of (3x5x8 =) 120 classes each with a characteristic wind deficit (%), and wake length (km). The characteristic values per class and per OWF are taken as time-averages throughout the WINS50 simulation duration, i.e., minimum, median and maximum wind deficit and wake length. The timeseries of wind deficit and wake length per OWF are determined as explained below.

Wind deficit determination

To determine the wind deficit at each OWF and each timestep of the WINS50 advanced wind farm wind simulation, the wake recognition algorithm follows these steps:

1. The wind deficit across the entire domain is determined by subtracting the wind fields between the WINS-CTL and WINS50 simulations. It is noted that small and irrelevant deficit values (<2%) may be attributed to numerical accuracy of the two simulations rather than the actual impact of offshore wind farms on the atmospheric layers. For that reason a minimum threshold of 5% wind deficit or surplus is accounted for.
2. All points across the domain are discretized (at each timestep) into the predefined wind speed, wind direction and atmospheric stability classes.
3. Per OWF and per simulation timestep, the predominant wind speed, wind direction and atmospheric stability condition is determined based on conditions calculated at all grid points within its polygon.

The same approach is followed to identify the wind deficit within the wake region downwind from OWF boundaries, following the wake length determination (see next). Therefore, a separate wind deficit is determined for the wake region outside the OWF polygon specifically.

Wake length determination

To determine the wake length at each OWF and each timestep of the WINS50 advanced wind farm wind simulation, a wake recognition algorithm is used that follows these steps:

1. Various wind farms are automatically clustered based on proximity and the respective polygons are merged, see Figure 2.1. This is necessary to avoid too many wakes extending within other OWF's (see also step 5 about treatment of data points that are boundary capped).
2. The wind deficit across the entire domain is determined by subtracting the wind fields between the WINS50 control and OWF scenario simulations. The wind deficit maps exclude the areas within the OWF polygons for the determination of the wakes.
3. The predominant wind direction within each OWF is determined by accounting all grid points within the respective wind polygon.
4. The predominant wake sector is searched within 20° (with a step of 1°) around the extended centreline from the predominant incoming wind direction (41 downwind transects), to account for slight deviations in the respective orientations. Under strongly stable conditions, wakes from large offshore wind-farm clusters have been observed and modelled to persist for more than 50 km, and in idealized large-eddy simulations even up to ~100 km downstream (Canadillas et. al, 2022). All transects are therefore

drawn in this study with a 150 km length measured downwind from the centroid of the OWF, with a spatial resolution of 750 m. The transect to represent the centreline of the wake is determined by searching the highest cumulative wake intensity, with higher weight assigned closer to the OWF boundaries.

5. The wake length is then determined by employing a low pass threshold of wind deficit at 5%, i.e., the wake length is either 150 km or taken equal to the distance along the predominant transect at which the wind deficit falls below 5%. It shall be noted that no analysed transect showed a wake persisting for the entire 150 km in the present analysis. In other words, the upper length threshold of 150 km (Step 4.) employed in the transect analysis is sufficiently large for the wake length analysis, as intended. If the wake length is capped due to crossing land and /or neighbouring OWF boundaries (before the deficit falls below 5%) then the wake length is not considered further in the classification process (data point is dismissed).
6. Within the wake polygon, the mean wind deficit is determined similarly as explained previously for the wind deficit within the OWF polygon.

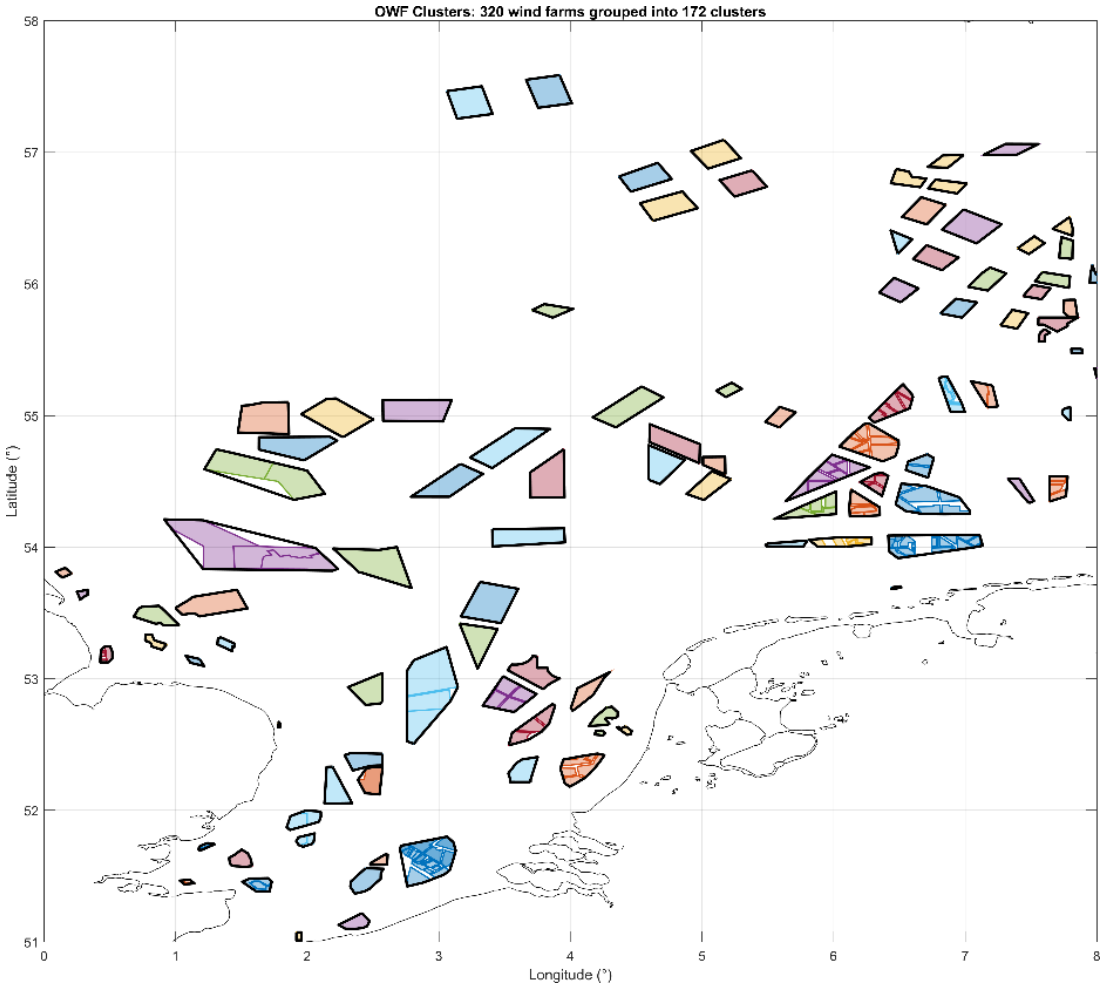

Figure 2.1 Clustering of windfarms based on proximity of respective centroids and merging of respective polygons to avoid excessive boundary capping of developing wakes.

The process for wake extraction is depicted for two of the OWF in the WINS50 domain and for the three first timesteps of the simulation period (in control and OWF influence respectively) in Figure 2.2.

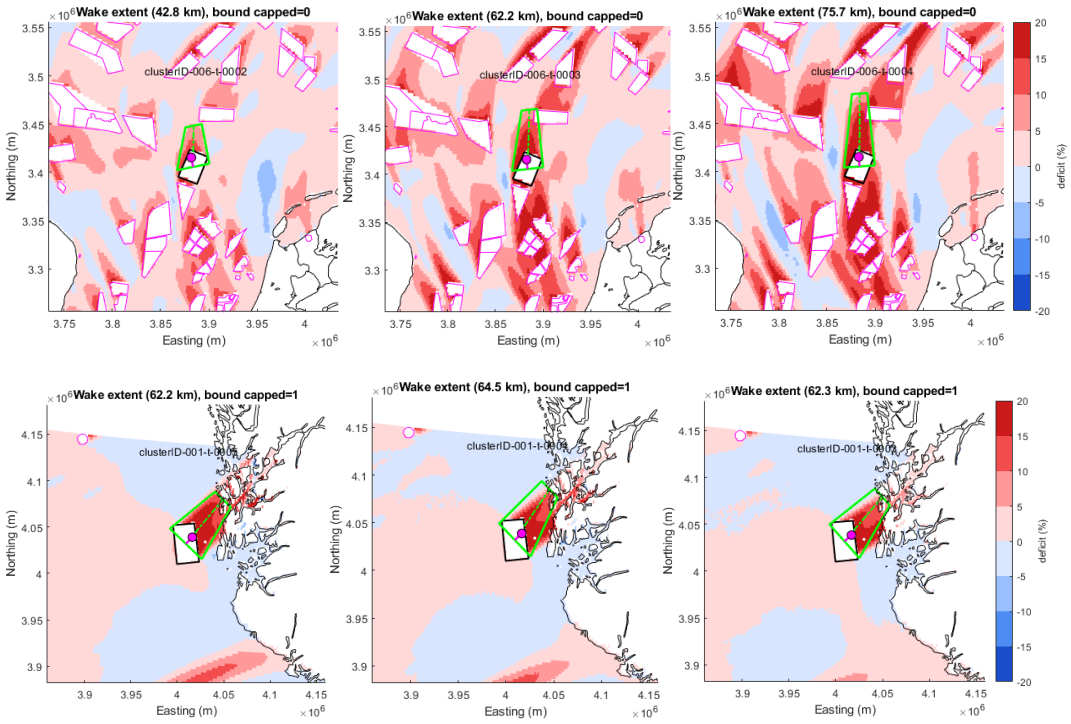

Figure 2.2 Wake detection for two wind farms within the modelled domain. Wind deficit within OWF and within land boundaries are masked out. The incoming wind direction is indicated by the magenta line (-o) drawn at the OWF centroid. The green dashed line (--) represents the identified predominant wake transect, the orientation of which may vary slightly compared to the incoming wind direction. The transects identified in the first OWF (top panels) are not capped by land or neighbouring OWF boundaries as opposed to the transects of the OWF below which are thus dismissed from further analyses.

Aggregation over OWF

This information can be retained at OWF level or aggregated across OWF's, depending the needs of each investigation. For aggregation, the OWF area (in km^2) appears to be the variable with the strongest correlation with wake length and wind deficit especially within the wake region (downwind from the OWF area), see example below (Figure 2.3 and Figure 2.4). Both wind deficit and wake length generally increases with increasing OWF area. This relation is most noticeable for wake lengths in specific. Based on this correlation and typically considered OWF areas, the following additional five OWF area classes are considered: i) 0-50 km^2, ii) 50-100 km^2, iii) 100-200 km^2, iv) 200-350 km^2, v) 350-Inf km^2. With the aggregation approach the wind deficit (within the OWF polygon and wake region) and wake length characteristics may be used for OWF's that are not within the WINS50 domain or scenarios.

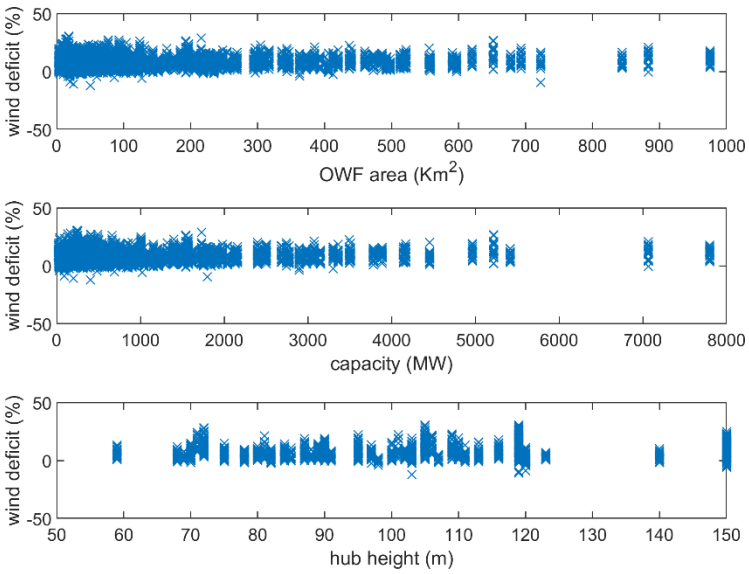

Figure 2.3 Example of the relation between the wind deficit (within OWF polygon) and various OWF properties, i.e., total area (top panel), capacity (mid panel) and hub height (bottom panel), for omnidirectional, unstable atmosphere and wind speeds between 2.5 and 20 m/s.

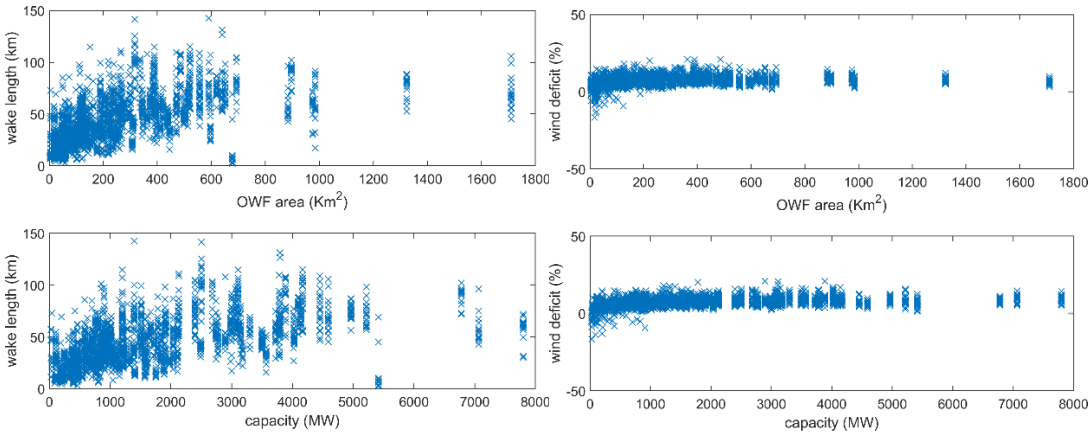

Figure 2.4 Example of the relation between wake length (left panels) wind deficit within wake region (right panels) and various OWF properties, i.e., capacity, total area and hub height, for omnidirectional, unstable atmosphere and wind speeds between 2.5 and 20 m/s. Plotting wakes against hub height information is not possible because for the extraction of wake lengths, and wind deficit within the wake region in specific, various OWF (with varying hub heights) were clustered, i.e., jointly considered to limit boundary-driven capping of wakes.

Obviously, this approach is not expected to resolve the influence of OWF's on atmospheric layers (and hence on waves and currents) as accurately as with the LES employed in WINS50 wind fields, however it is a further advancement in implicitly resolving relevant processes compared to the crude constant and uniform wind speed reduction employed within OWF polygons, used in earlier modelling efforts.

2.3 Wind deficit and wake length classification results

Figure 2.5 and Figure 2.6 present the results of this classification algorithm for all OWF's, irrespective of OWF area, using as input the WINS50 domain and the WINS50 control and wind farm simulation of the atmospheric layer. The further breakdown of classification results per OWF area class is presented in Appendix A.

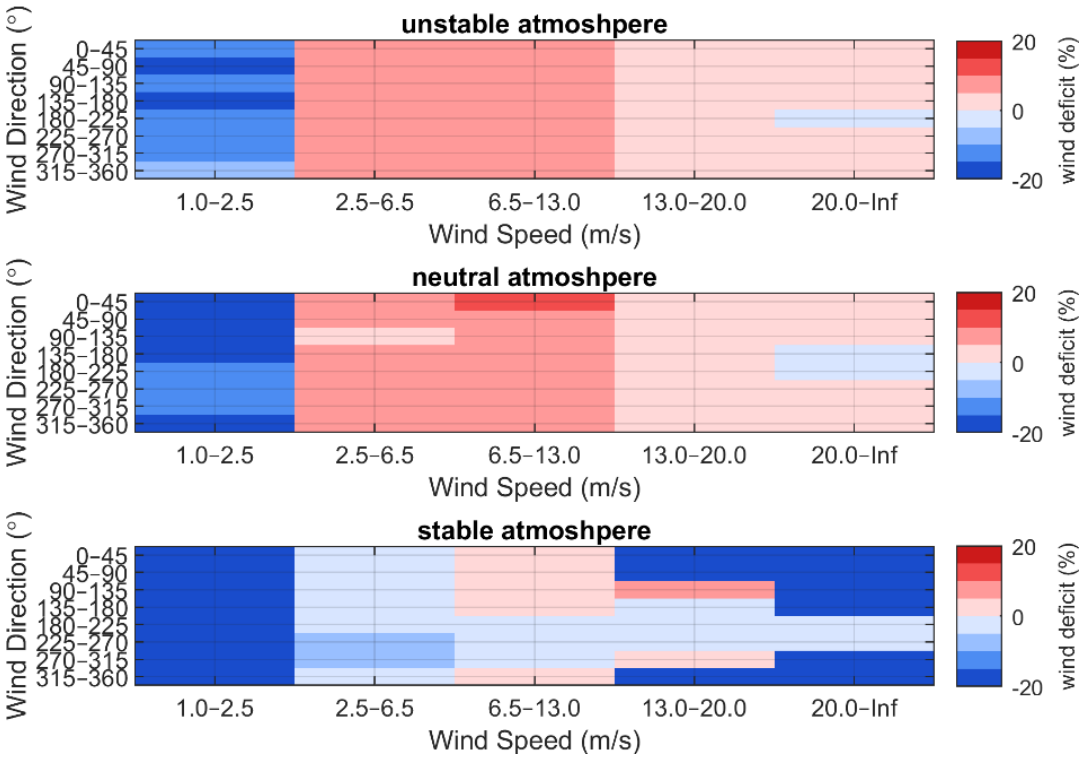

Figure 2.5 Wind speed deficit within OWF for the various predefined classes. Negative deficit denotes a surplus of wind (higher wind speeds in the presence of OWF's). Median value across all OWF's (irrespective of area). Per OWF, the mean wind deficit value of all considered timesteps within respective class is accounted for.

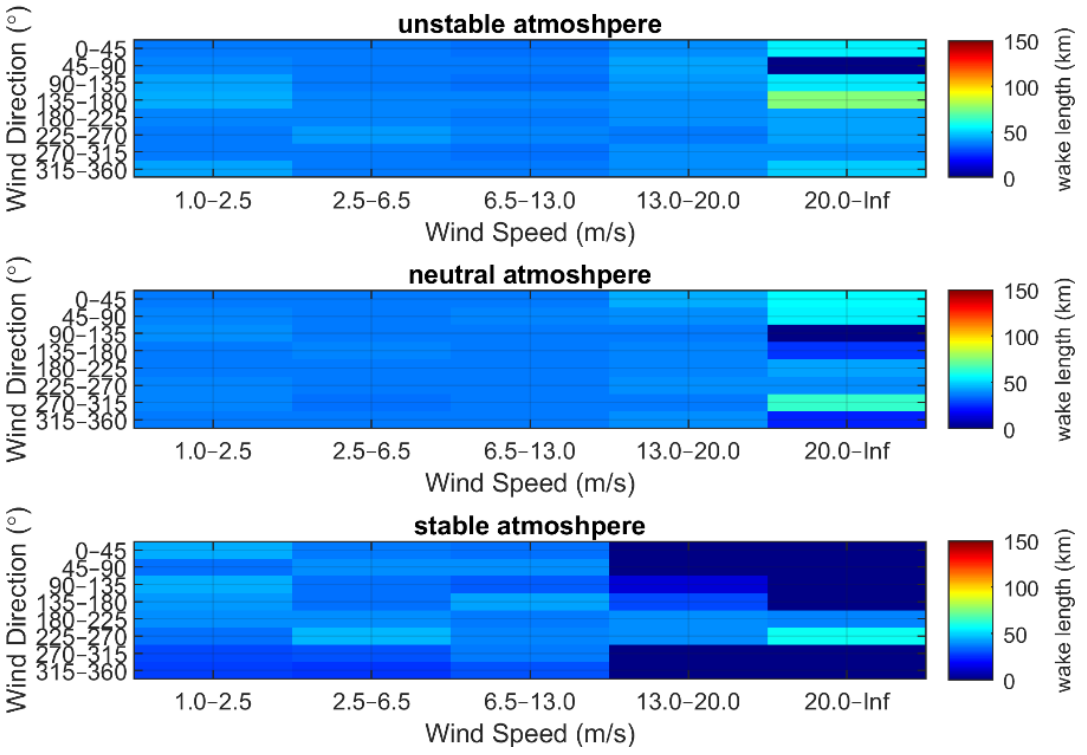

Figure 2.6 Downwind wake length for the various predefined classes. A maximum of 150 km is considered. Median value across all OWF's (irrespective of area) is displayed. Per OWF, the mean wake length value of all considered timesteps within respective class is accounted for.

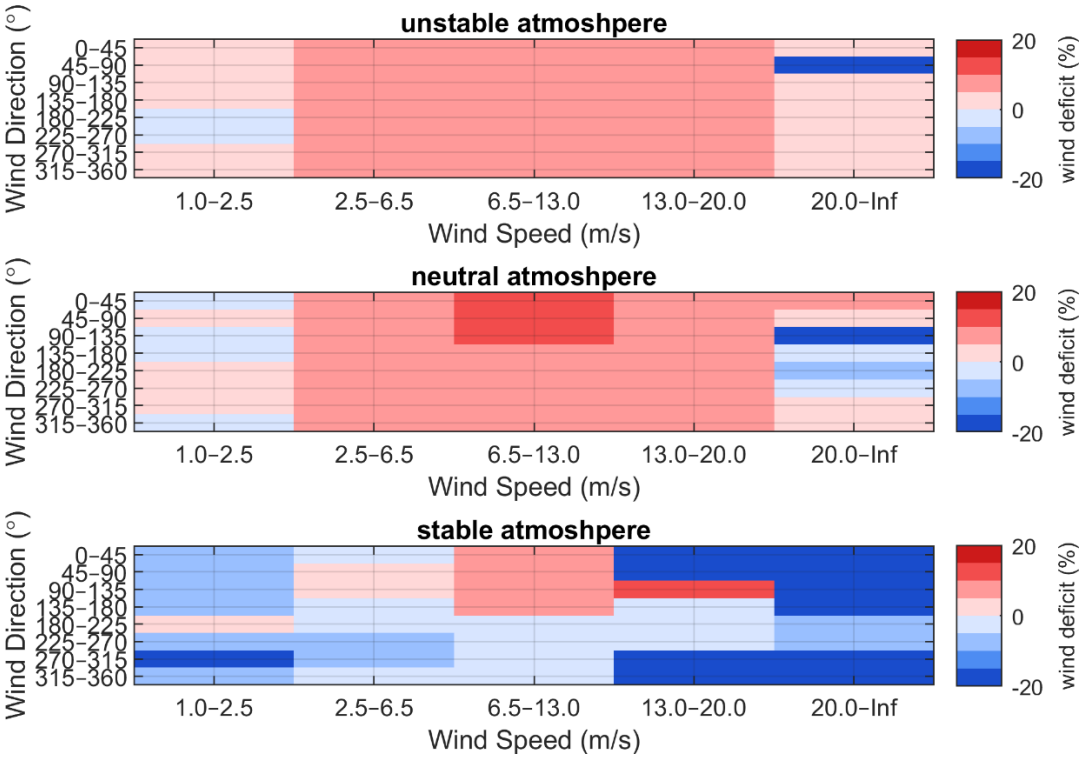

Figure 2.7 Wind speed deficit within the wake region (see green polygons in Figure 2.2) directly downwind from OWF for the various predefined classes. Negative deficit denotes a surplus of wind (higher wind speeds in the presence of OWF's). Median value across all OWF's (irrespective of area). Per OWF, the mean wind deficit value of all considered timesteps within respective class is accounted for.

The results of the classification algorithm are in line with expectations.

- Wind deficit above cut-in speeds (U_{10} >2.5 m/s) is in the order of 5-15%. It is noted that a 10% constant and uniform wind speed deficit is applied within the OWF's in the crude schematization approach, so in that regards the two approaches are roughly aligned.
- The wind deficit percentage (not absolute value) generally reduces with higher wind speeds.
- A wind surplus is noted for various wind speed and direction classes under stable atmospheric conditions, as expected, due to downward transfer of momentum by the rotating blades.
- In Appendix A, it is shown that the wind deficit generally increases with increasing offshore wind farm area.
- The wake length never exceeds and rarely approaches the predefined threshold value of 150 km. Wake lengths are mostly between 10-70 km, irrespectively of the atmospheric conditions.
- Wake lengths show a strong correlation with the OWF area, larger OWF's have larger wake lengths (see also Appendix A).

2.4 Generation of synthetic wind fields

The developed method has been used for the generation of synthetic wind fields to model and assess offshore wind farm influence on atmosphere, waves and currents, using the ERA5 surface wind fields as a starting point. In principle, using the model and the ERA5 data, synthetic wind fields with OWF effects can be generated any location around the world and for any offshore wind farm polygon considered. The two main characteristics extracted from the classification, i.e., wind deficit within OWF polygon and wake length, both as a function of wind speed, wind direction, atmospheric stability and offshore wind farm area has been applied on the ERA5 dataset to generate synthetic wind fields as follows:

1. The baseline ERA5 wind fields across the entire domain are discretised into the same 120 classes as mentioned above for all individual timesteps of the considered simulation period.
2. Each of the OWF in the considered operational scenario, is then classified by the predominant wind speed, wind direction and atmospheric stability within one of the 120 classes for each timestep.
3. Depending the area of the OWF and the respective class, at each timestep a condition dependent uniform wind deficit factor is applied on the (non-uniform) base case wind field, in line with the values presented in the classification matrices, see e.g., Figure 2.5.
4. Directly downwind of the predominant wind direction, the wind deficit may be applied with a certain profile along the wake length identified in the classification algorithm. The Jensen (Park) model or the Bastankhah-Gaussian model are commonly used at turbine level for determining a wake profile. These can also be adapted to a meso-scale (wind-farm level) by averaging turbine-level effects spatially across the farm. In this case, we opted for a more simple conical wake profile[1] with a uniform and condition- and wind farm area- dependent uniform wind deficit factor (see Figure 2.7) applied within. Further improvements are possible in future updates of the current study.

With this approach, and cumulating all OWF's in consideration, a 'calibration matrix' is generated for each timestep to be applied on the ERA5 wind fields. Figure 2.8 presents as example for a few moments in time the wind wakes, to be applied on the standard wind field. This calibration matrix goes further than the constant and uniform wind speed reduction of 10% and only within the OWF polygon as applied previously.

The final outcome is a synthetic wind field that has a semi-advanced schematization of the influence of OWF's on the surface winds, yielding at least from a physical point of view an improvement compared to the crude 10% reduction employed earlier. The performance of this schematization may vary across different locations. Hereby, it is presented simply by means of timeseries of wind speed (wind directions are unchanged) at one location within a randomly selected OWF. For that location, the WINS50 - WINS-CTL wind deficit (assumed as ground truth) is compared with ERA5-OWF1 wind deficit (10% constant and uniform reduction) and ERA5-OWF2 (semi-advanced approach accounting for wind speed, wind direction and atmospheric stability condition, including wakes downwind from the OWF). The timeseries comparison can be found in Figure 2.9, while relevant statistical values may be found in Figure 2.10. There is a fair correlation between the respective timeseries, rmse and std values are within reasonable bounds and bias is limited.

In conclusion, in this chapter we present the development of a physics-based parametric method to add the OWF effects by means of post-processing to the undisturbed surface wind fields. The first results look promising and already yield an advancement compared to the previously employed crude method of 10% constant and uniform wind speed reduction, but further optimization and verification is still necessary in future steps of this study.

[1] The wake polygon narrows linearly from its initial half-width to 50% of that width over the wake length, corresponding to a lateral slope of 1:2 on each side (i.e., for every unit of downwind distance, the wake edge contracts by 0.5 units). The half-width is defined as half of the offshore wind farm's perpendicular extent (relative to the incoming wind direction), which sets the initial left–right boundaries of the wake at the farm's downwind edge.

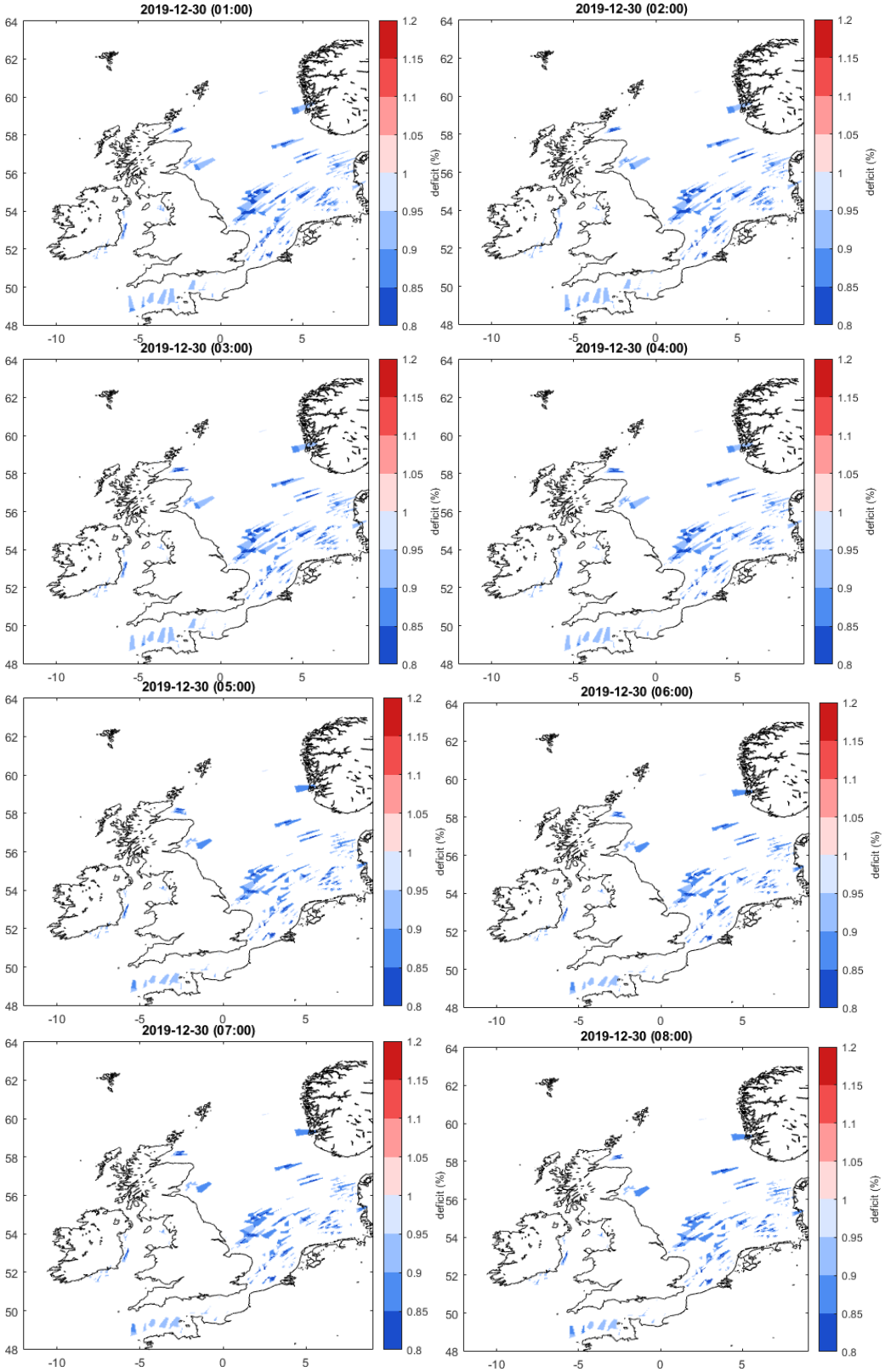

Figure 2.8 Calibration factors to be applied on ERA5 wind fields for synthetic wind field generation based on the classification algorithm results across the study area accounting for all OWF's in the WINS50 scenario.

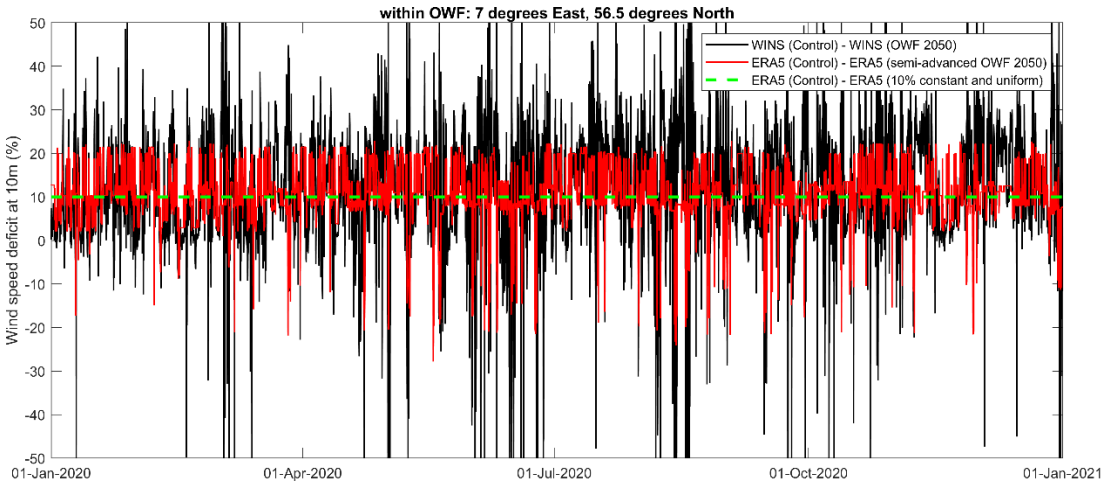

Figure 2.9 Wind deficit (%) timeseries comparison between WINS50 / WINS-CTL, ERA5 Semi-Advanced / ERA5 and 10% constant and uniform deficit for the 2020 simulation year.

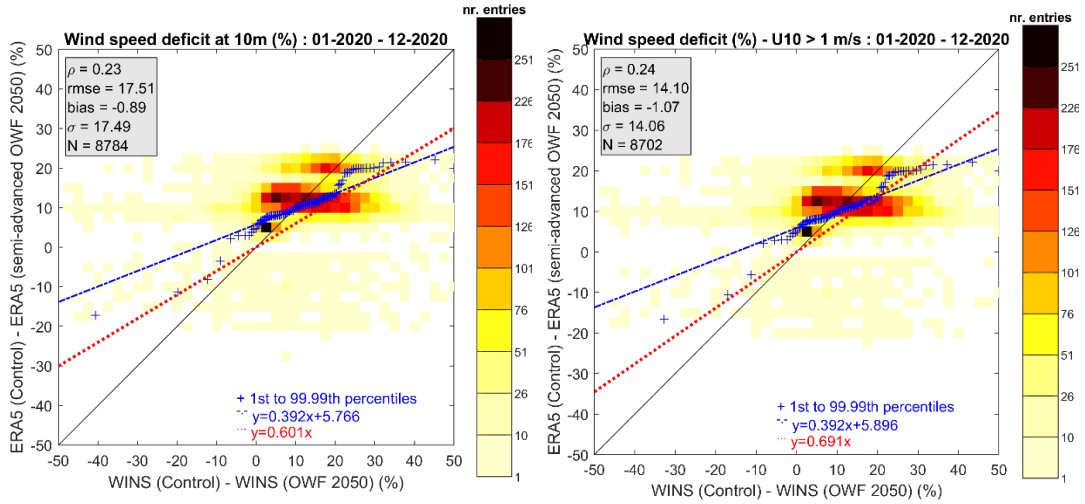

Figure 2.10 Wind deficit (%) scatter plot comparison between WINS50 / WINS-CTL, ERA5 Semi-Advanced / for the 2020 simulation year for a single example location within an OWF polygon (7 degrees East, 56.5 degrees North). Left: all data. Right: only data with $U10_{CTL}$ > 1/ms.

3 Method dependencies

This part of the study focuses on the dependence of the OWF's effects on the hydrodynamics and waves on different variables, for example location with relation to the wind farms, atmospheric stability, wind speed and wind direction.

3.1 Modelling approach

This study uses the results from the recent hydrodynamic and wave modelling performed for WOZEP research program with the use of the extensively calibrated 3D Dutch Continental Shelf Model – Flexible Mesh (3D DCSM-FM; Zijl et al., 2023, 2024) model and DCSM-SWAN (Zijl et al., 2021) spectral wave model. The original research for which the modelled data were created studied the wind wake effects of OWF's on hydrodynamics (Zijl and Leummens, 2024) and waves (Gautier and Caires, 2015) regarding three different OWF effect parametrisations:

- A "reference" simulation: hindcast of the 2020 year, where no effects from OWF's are included.
- A "basic" wind schematization of the OWF effects: in which the effects of the hypothetical OWF by 2050 are captured through a uniform and constant 10% reduction in ERA5 wind speeds within the OWF polygons (directions remain unchanged).
- An "advanced" wind schematization of the OWF effects: in which the effects of the hypothetical OWF's by 2050 are captured by the physically-based simulated wind fields of the year 2020 (involving extraction of momentum, mixing and blockage) from the WINS50 dataset by KNMI, thus additionally including the wake effects of OWF's.

The fields generated with the method described in the previous chapter are not considered in this assessment. The basic and advanced simulations use the reference 2020 hindcast model as a basis. This means that all other forcings, numerical settings and boundary conditions are identical to those employed in the reference simulation. Consequently, by comparing the model results of scenario and reference simulations only the effect of the varied wind input is assessed.

Note that the effect of each OWF in the hydrodynamic model is defined not only through its effect on wind but also through the drag of the monopiles of the Wind Turbine Generator (WTG). The OWF monopiles are represented in the 3D DCSM-FM model as vegetation fields with a certain stem density, diameter and infinite stem height. In this parameterisation, the monopiles cause a sink of momentum leading to a local reduction in the current. The extracted momentum loss is released as an increased level of turbulent kinetic energy. This method is similar to theFitch et al. (2012) wind farm parameterization that is used to include the effect of monopiles in the WINS50 wind model.

3.2 OWF's effects on flow

In this study the OWF's effect on the flow, is defined as the current velocity difference between advanced and reference model runs. The variables to check its correlation with are:

- wind speed
- wind direction
- atmospheric stability factor derived as temperature difference between air and water
- distance from shore
- distance and placement relatively to the OWF's

OWF's spatial effect across the southern North Sea was assessed through a correlation parameter coefficient 'a' (symmetric slope; change of 0.01 represents ~1% change in the value) between modelled current velocity values for the two scenarios. This coefficient is determined as a multiplier term in relation: *(Adv) = a * (Ref)*. Alternatively, more advanced representation of the similar relation can be described by 'b' and 'c' parameters in: *(Adv) = b * (Ref) + c*. Due to restrictions in the availability of the spatial modelling results, the analysis of the OWF's effects on the flow throughout the 3D DCSM-FM domain is performed based only on daily instantaneous values.

The analysis of OWF's effect on a set of predefined locations is enhanced based on the findings from the previous report (Deltares, 2025). It is focused on the visual representation of the relations between the OWF-induced current velocity difference and the list of various parameters presented above.

Hourly current velocity values are used in the analysis, however only the peak velocities per tide are considered. The selection of the peak current velocity values is done via the search for the local maximum values with approximately a half tidal cycle separation period. This results in 2 values per tidal cycle which are considered together without distinction for the varying current direction.

3.3 OWF's effects on waves

The effects of OWFs on waves are drawn from the comparison of modelled wave parameters between the "Reference" wind and the two wind schematizations (Basic -ERA5 with constant and uniform 10% U10 reduction- and Advanced -WINS50-) that reflect OWF's influences on wind fields.

4 Flow – where do the OWF effects depend on?

4.1 Introduction

In this section, the OWF's effect on the current velocity is studied in terms of its dependence on various parameters of the wind and atmosphere. The main indicator for these effects is defined in this study as the difference in modelled current velocity values between the "reference" and "advanced" wind scenario simulations. The analysis uses data from the modelled period of one year. Spatial flow data used in this study is only available with daily resolution, while data at the stations analysed below have hourly resolution (Figure 4.1). The full list of studied locations is: WALCRN2-70, NOORDWK2-70, EURPFM, LICHTELGRE, STRAINS M18, IJGL MP19, HKWA and HKWB.

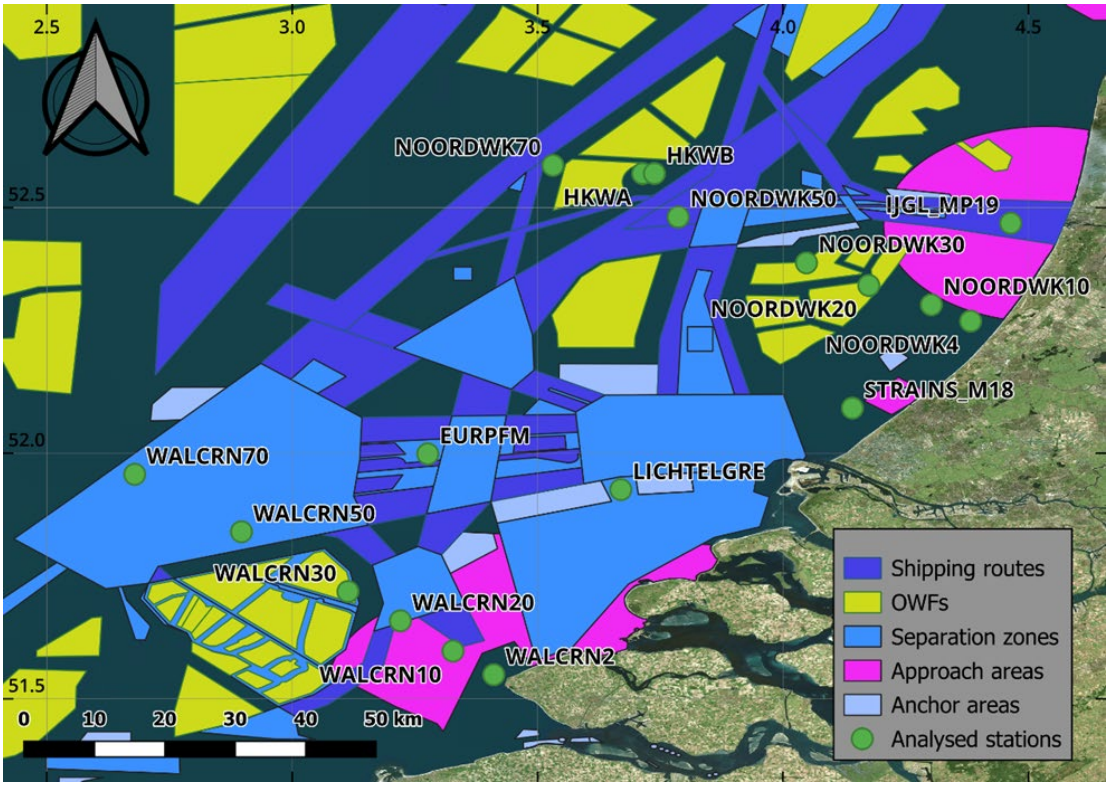

Figure 4.1: Stations analysed for OWF effect on hydrodynamic parameters.

In the previous analysis report (Deltares, 2025), statistical parameters of the OWF's effect were determined for the same stations. In this study, analysis builds upon those findings and extends the assessment of the relation between the OWF's effect and meteorological situation with awareness of the local configuration of the wind farms system at each of the studied locations. The considered parameters are the distance to the wind farm location and meteorological parameters such as wind speed, wind direction and atmospheric stability (unstable, neutral, stable atmosphere).

4.2 Spatial effects of OWF's on currents

In the previous study (Deltares, 2025), OWF's effect at selected stations was assessed through a symmetric slope coefficient 'a' (change of 0.01 represents ~1% change in the value) between modelled current velocity values for the two scenarios. This coefficient can be determined as

a multiplier term in relation: *(Adv) = a * (Ref)*. Alternatively, more advanced representation of the similar relation can be described by ‘b’ and ‘c’ parameters in: *(Adv) = b * (Ref) + c*.

Figure 4.2 presents spatial distribution of the symmetric slope across the southern North Sea showing clear area of effects imposed by the OWF operation. The revealed pattern shows that the effect on current velocity varies spatially from negligible up to 20%. The highest OWF effects are localised within wind farms limits, however for certain OWF installations an evident wake effect can be observed. The latter points at a dependency of the imposed effects on the OWF’s parameters such as turbine power and total OWF power, monopile density or width.

While the majority of the Dutch coast and navigational channels are lying within the area where the maximum expected change in current velocity does not exceed 5%, the Dutch far offshore navigation area and northern parts of Dutch separation zones and navigational routes next to the unnamed future wind parks (<4ºE) have areas with larger effects with up to 20% change estimation.

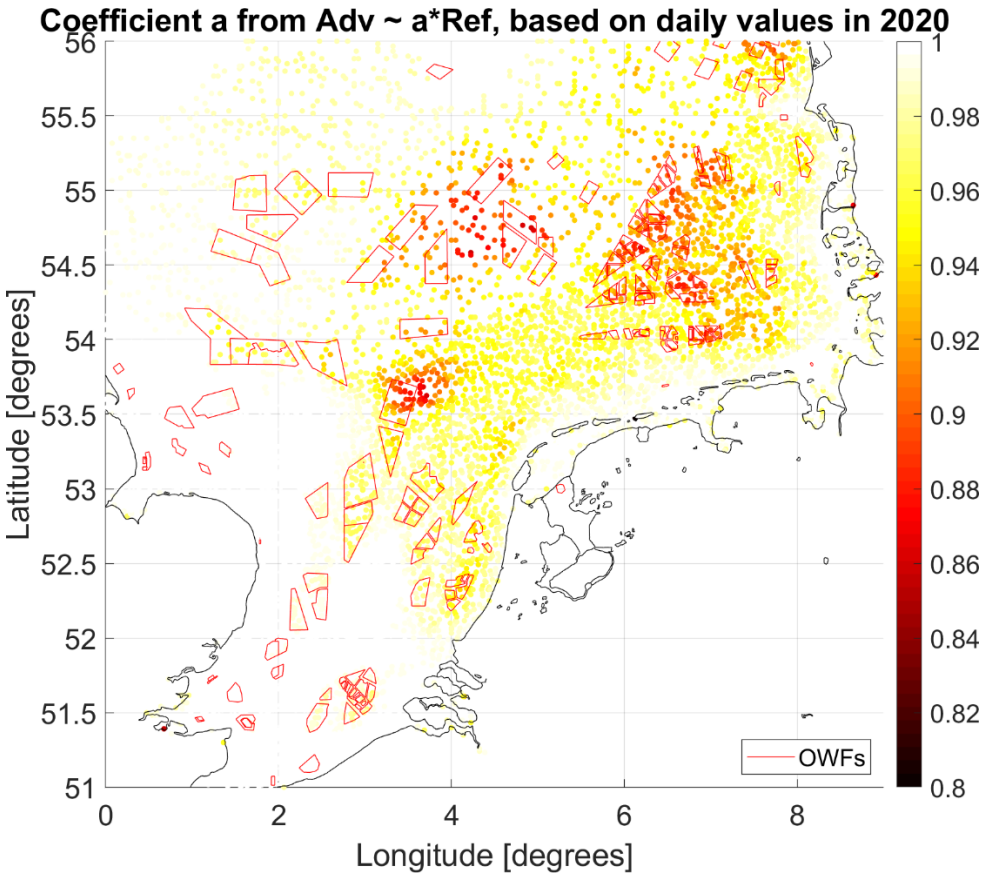

Figure 4.2: Symmetric slope between the current speeds with and OWF effects (the situation with (‘Adv’) and without (‘ref’) OWF’s).

Similar patterns regarding increase of potential OWF’s effect inside of wind farms themselves as well as in leeward side of wind parks, and deep waters is observed for ‘b’ and ‘c’ parameters of the relation between Reference and Advanced scenarios (Figure 4.3). It’s important to note that the sign of ‘c’ parameter or position of ‘b’ coefficient against 1.0 value does not directly correlate with the awaited sign of potential change in current velocity.

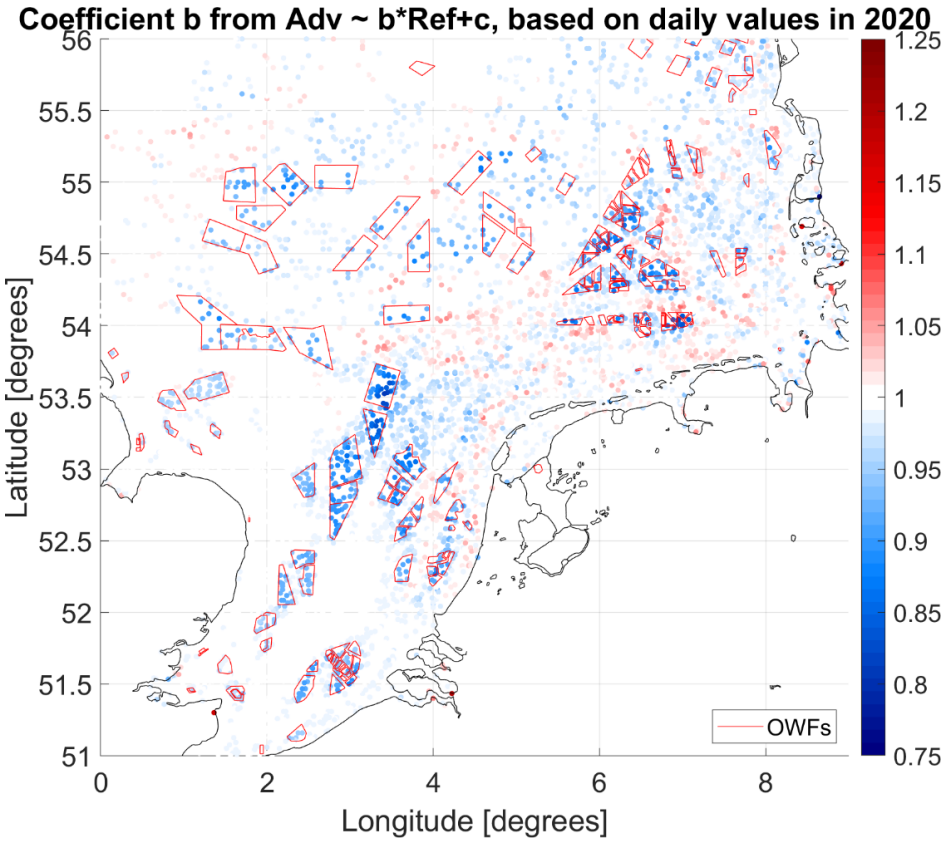

Figure 4.3: Parameter 'b' of the situation with ('Adv') and without ('ref') OWF's

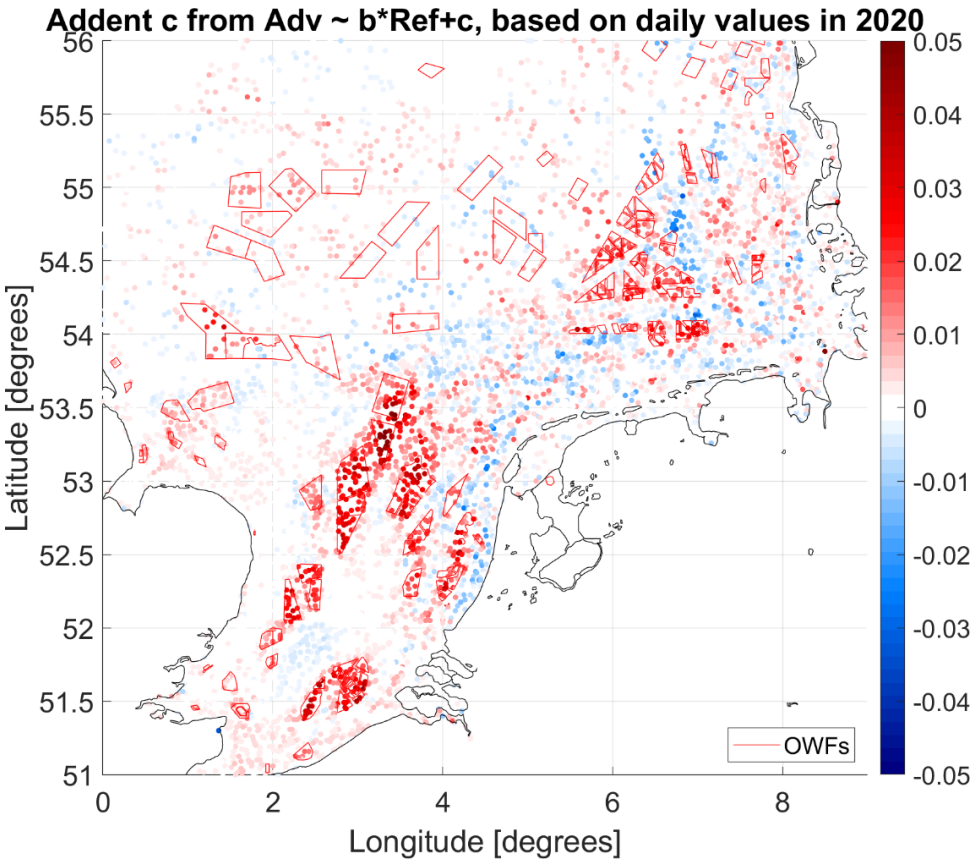

Figure 4.4: Parameter 'c' of the situation with ('Adv') and without ('ref') OWF's

4.3 Effects of OWF's on flow for predefined locations

For predefined output locations, hourly modelled flow velocities are available, with and without OWF's for an entire modelled year. The effect of the OWF's is defined as the difference between the flow velocity with OWF minus the flow velocity without OWF. In this paragraph we try to find out if there is a relation or a dependency between this effect and wind speed, wind direction or atmospheric stability. Only the peak velocities per tide will be considered (2 values per tidal cycle). The selection of the peak current velocity values was performed as the search for the local maximum values with approximately a half tidal cycle separation period. This approach left approximately 1430 values in the further described analysis which allowed for a sufficient confidence in the resulting conclusions. When considering the current differences, it is good to have some idea of the undisturbed peak tidal velocity values. On average these are some 0.8 m/s with minima and maxima of some 0.4 and 1.4 m/s.

Here, the summary of findings based on the analysis of all available stations is presented. An example plot of the relations and dependencies is given for each of the analyses for a single station while all other stations' plots are present in Appendix B.

4.3.1 Effect of OWF's on flow, related to wind speed (see also Appendix B.1)

In Figure 4.5 - Figure 4.7 the effect of the OWF's on flow velocity is presented as function of wind speed, each for one location. The cloud of dots shows wide spread indicating that the effect is not strongly (linearly) depending on the concurrent wind speed. Some local effects can still be observed, such as for NOORDWK50 where the effect of the OWF's appears to be larger in range of 5-10 m/s wind speed indicated by larger spread in current velocity difference. However, with so much spread, the relevance of the fitted lines is very limited. The colours in these plots indicate the wind direction or atmospheric stability (defined as the difference between water temperature and air temperature). Since the colour distribution turns out rather random, there is no clear relation on these locations between the effect of the OWF's on flow and the wind direction. Also the atmospheric stability does not show correlation with the flow effect of the OWF's.

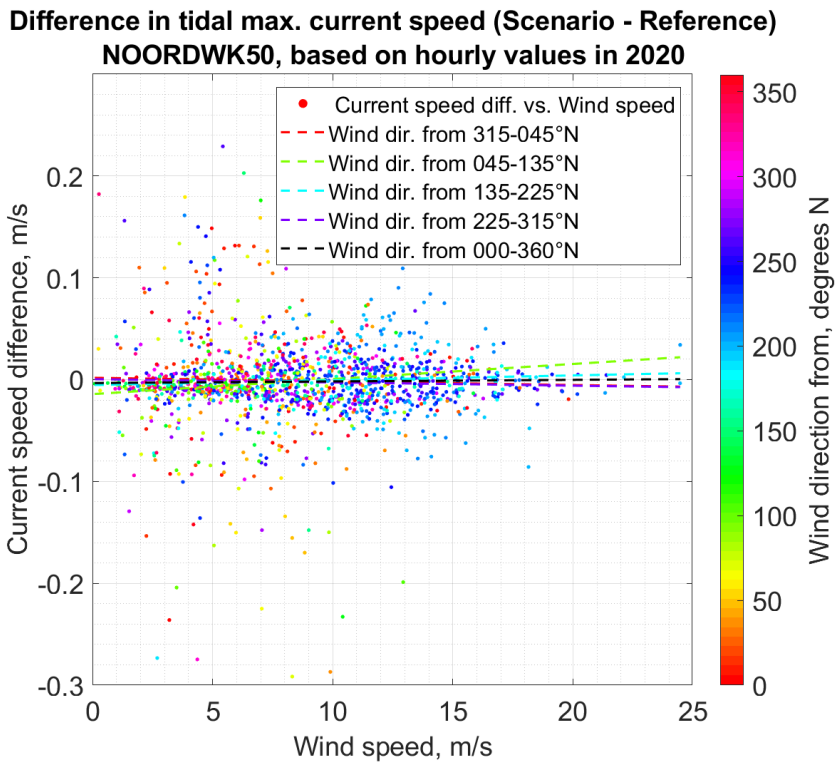

Figure 4.5: The effect of OWF's on flow (Y-axis) as a function of wind speed (X-axis) for various wind directions (colour) at location NOORDWK50 (~50 km from shore)

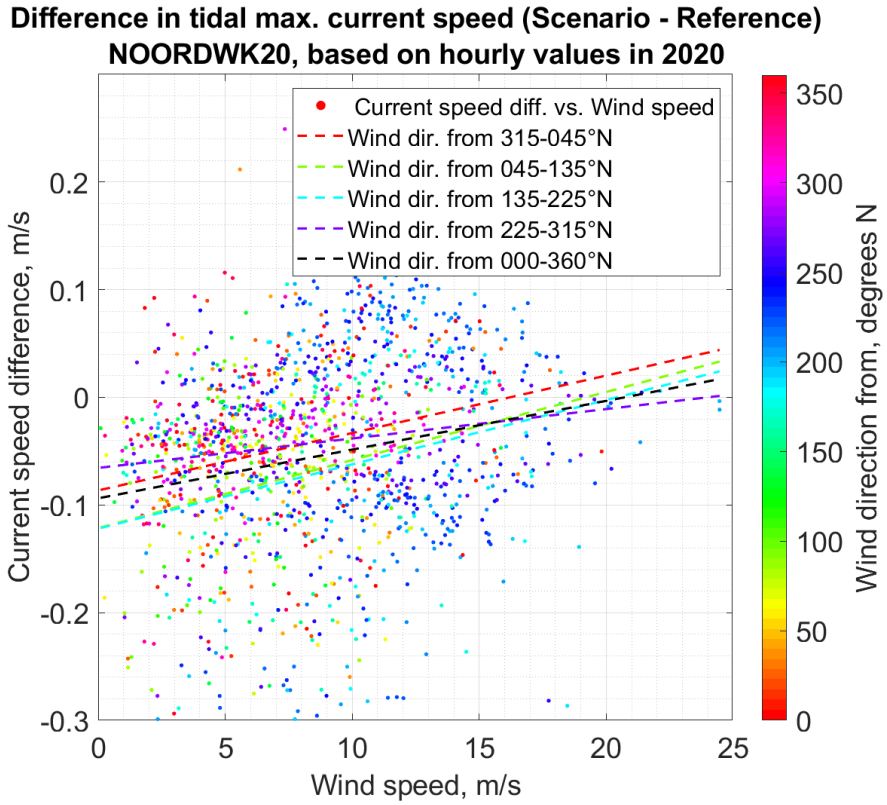

Figure 4.6: The effect of OWF's on flow (Y-axis) as a function of wind speed (X-axis) for various wind directions (colour) at location NOORDWK20 (~20 km from shore)

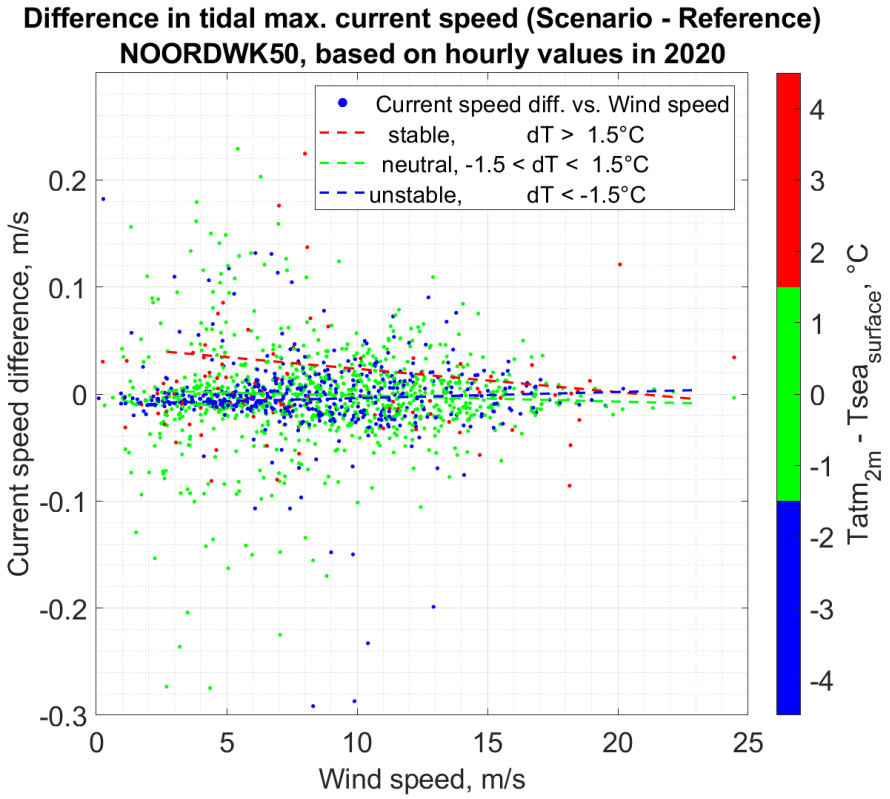

Figure 4.7: The effect of OWF's on flow (Y-axis) as a function of wind speed (X-axis) for various atmospheric stability conditions (colour) at location NOORDWK50 (~50 km from shore)

4.3.2 Effect of OWF's on flow, related to wind direction (See also Appendix B.2)

Comparable to the previous figures, Figure 4.8 shows per location the effect of the OWF's as function of wind direction. Now the colours represent the wind speed. The grey vertical bands indicate the wind directions for which the considered location is somewhat sheltered by an OWF. So typically the wind directions for which the effects would be more dominant (more negative current speed differences). However, this is not clearly visible within one plot, but per location we do see that for instance that the flow reduction at the entirely 'grey' NOORDWK20 is indeed larger than a rather 'white' location as WALCRN2, see Appendix B.2.

The main message here is again that there is no clear relation between the effect that OWF's have on flow on one hand and the wind direction on the other. For some locations we see that for wind directions of roughly 225ºN (SW) and 45ºN (NE) the difference in flow effect is somewhat larger than for other directions, see for instance WALCRN30, EURPFM and STRAINS M18. But these larger effects (=flow differences due to OWF) are somehow both negative and positive. It is unclear why.

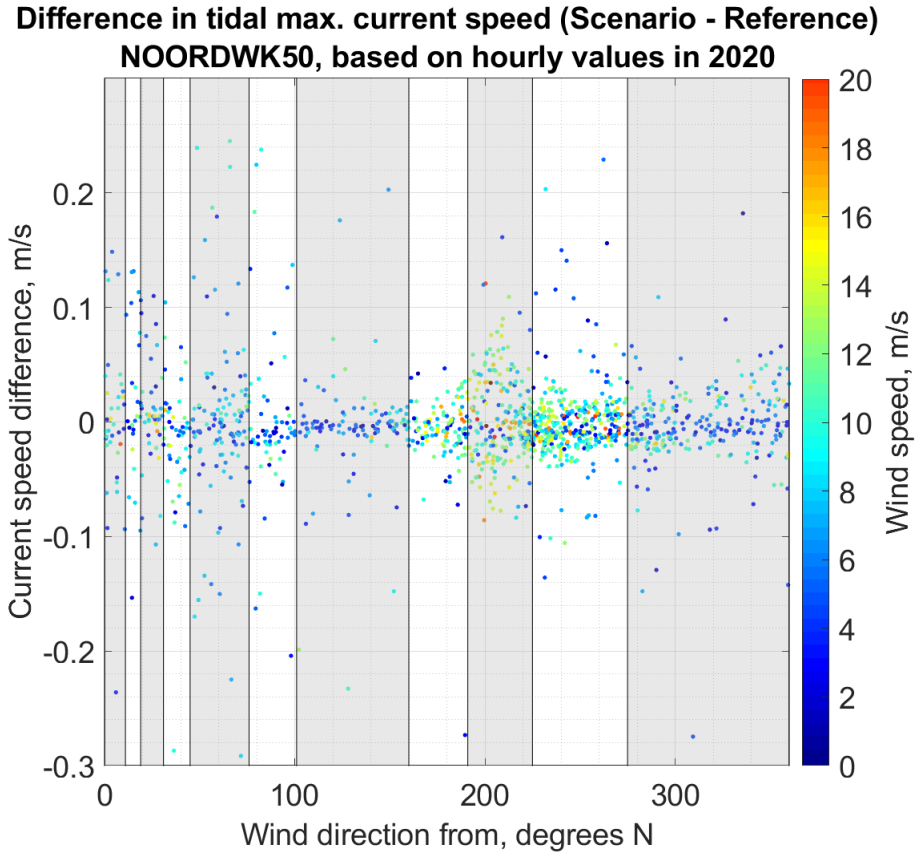

Figure 4.8: The effect of OWF's on flow (Y-axis) as a function of wind direction (X-axis) for various wind speeds (colour) at location NOORDWK50 (~50 km from shore). The grey areas indicate the directions at which the closest wind parks are located

4.3.3 Effect of OWF's on flow, related to wind speed and location.

The black dashed line in the panels of Figure 4.9 (Noordwijk) and Figure 4.10 (Walcheren) present per location the difference in current velocity between the situation with and without OWF's. The horizontal axis does not relate to time but just to the order of the difference in current velocity. These plots show that the difference is mainly zero, that the max flow increase (~0.25 m/s) is larger than the max flow decrease (~-0.5 m/s) and that this view slightly differs per location. The Noordwijk ray (the numbers in the location names refer to their distance from shore) shows larger differences than the Walcheren ray.

The colours indicate the associated wind speed. Whilst in most panels the colours seem to be randomly distributed, meaning that there is no relation between the effect of OWF's on flow and the wind speed, the panels of NOORDWK20 and NOORDWK30 and also WALCRN30 (these are located within the wind farms) show some order: The middle part is quite yellow, the outer edges more red. This implies that larger flow effects (both increase and decrease due to OWF's) occur with stronger winds. Especially the left side of these panels is red, indicating that the larger increase in flow velocity due to the presence of OWF's, occurs during moments with stronger winds.

But again, the main message is that there is no clear relation between the effect of the OWF on the flow velocity and the wind speed.

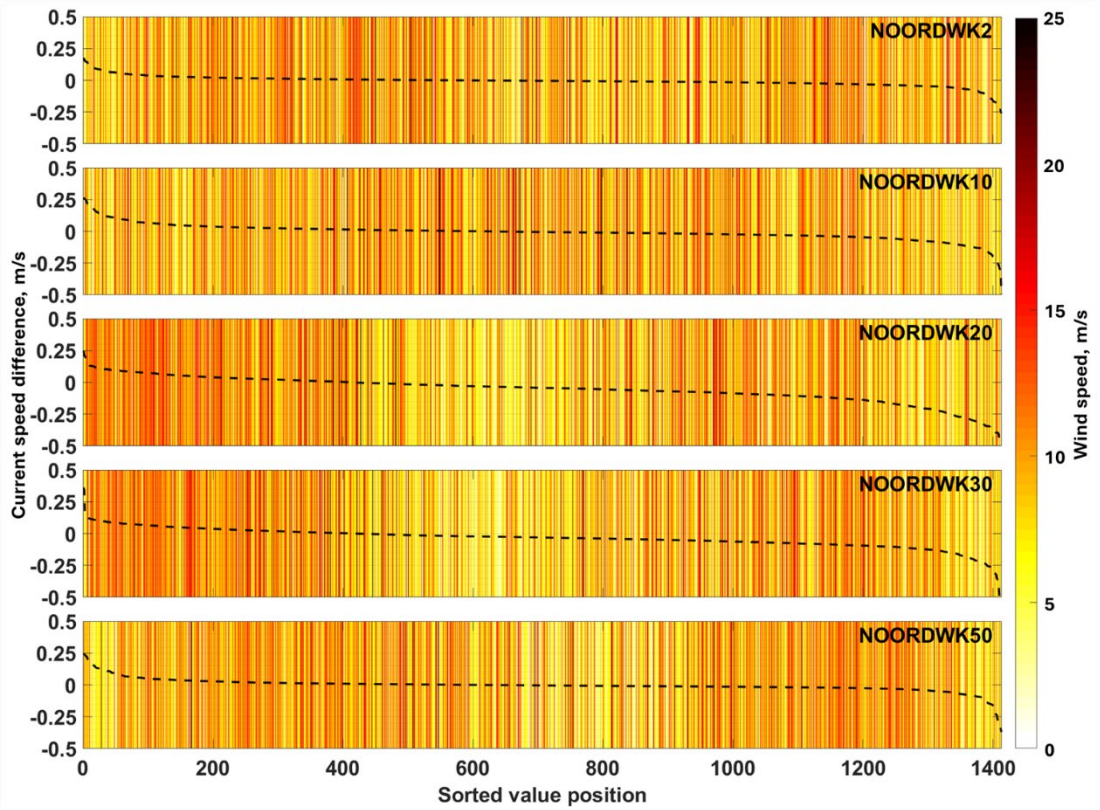

Figure 4.9: Current speed difference (with – without OWF) ordered from large difference to small (black dashed line) and synchronically occurring wind speed for NOORDWIJK locations

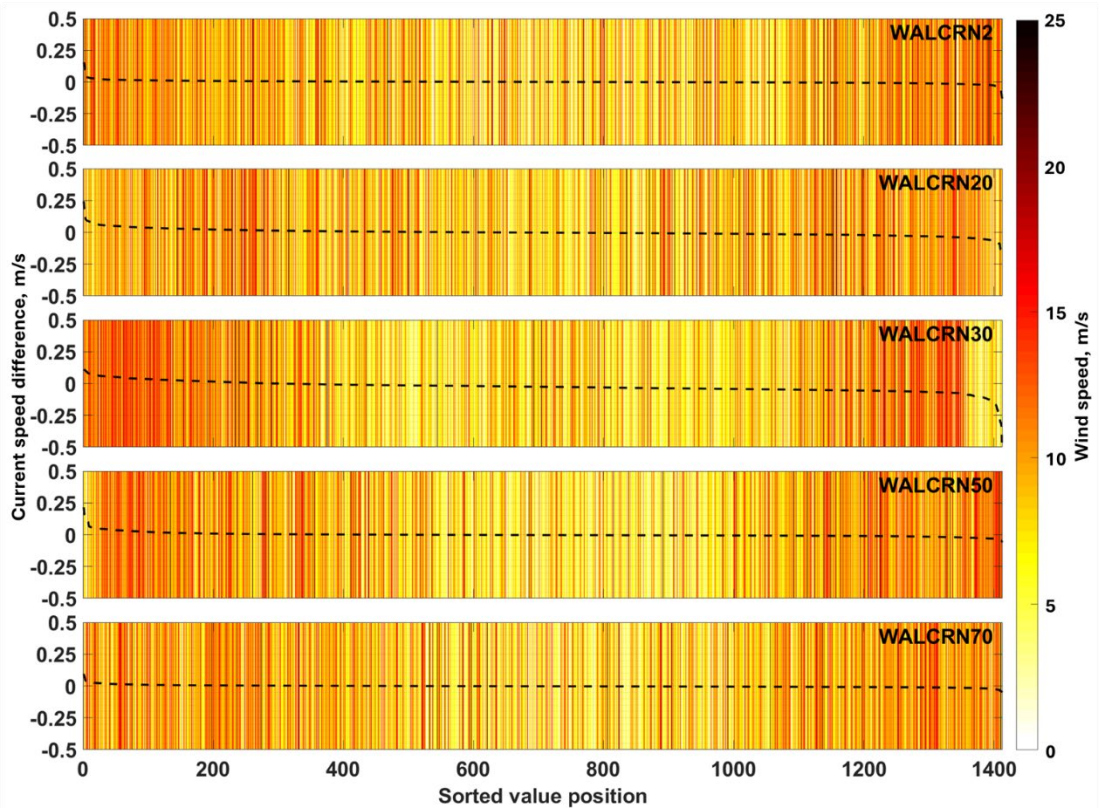

Figure 4.10:Current speed difference (with – without OWF) ordered from large difference to small (black dashed line) and synchronically occurring wind speed for WALCHEREN locations

4.3.4 Effect of OWF's on flow, related to location.

Figure 4.11 and Figure 4.12 present a statistical representation of the current velocity differences due to OWF's. Here, the effect of the distance to OWF's can be clearly seen both in dominating reduction of the current velocities and the increase of the current velocity difference variation. See Figure 4.1 for the position of the locations and of the OWF's.

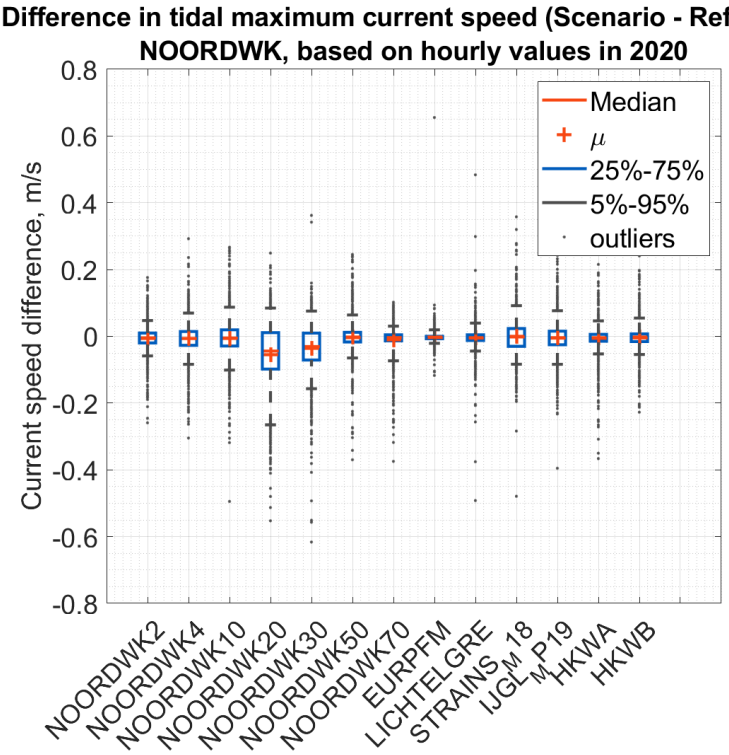

Figure 4.11: Box plots of current speed difference (with – without OWF) for various locations near the Noordwijk ray (see Figure 4.1 for locations)

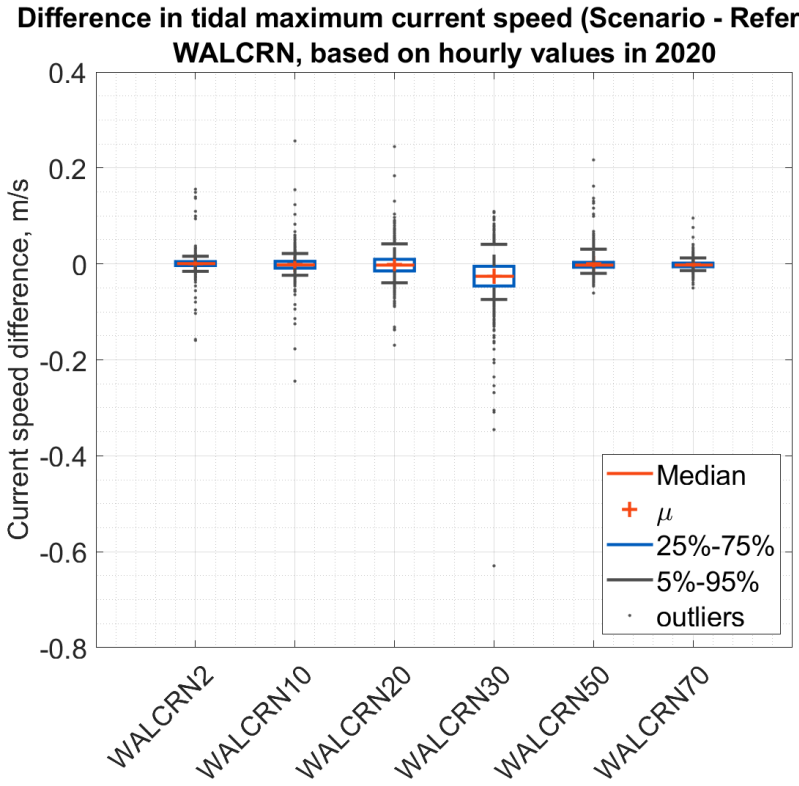

Figure 4.12: Box plots of current speed difference (with – without OWF) for various locations near the Wacheren ray (see Figure 4.1 for locations)

5 Waves – Extension of statistical analysis

5.1 Introduction

In this section, the effects of OWF's on waves and navigation are shown in terms of linear statistical parameters[2]. These are drawn from the comparison of modelled wave parameters between the "Reference" wind and the two wind schematizations (Basic -ERA5 with constant and uniform 10% U10 reduction- and Advanced -WINS50-) that reflect OWF's influences on wind fields. In this section we will discuss only the Advanced wind schematization (WINS50) which is deemed most representative. The statistical comparisons reflect the entire modelled period of one year in all three simulations. Moreover, the relevant locations are not assessed individually but rather clustered with respect to proximity to OWF (within and surrounding OWF) and to navigational features i.e. (far offshore) shipping areas, anchor zones and (port and inland navigation) approach areas. Regarding the proximity to the OWF, locations up to a distance of roughly 10 km from the OWF boundaries were considered[3]. It is noted that only locations within the Dutch EZZ are processed. The most relevant of the clusters analysed are presented in the remainder of this section and summarized in Table 5.1 and Figure 5.1.

Table 5.1 Clusters of offshore locations determined for the statistical analysis of OWF's effects on waves.

Cluster name	Description	# model output points
Dutch OWF's	Offshore locations within the Dutch OWF's (2050 scenario)	716
Surrounding area Dutch OWF's	All offshore locations that fall within roughly 10 km from the boundaries of OWF's	1358
Designated shipping routes	Offshore locations within the designated shipping routes (including separation zones) that fall within roughly 10 km from the boundaries of OWF's	385
Far offshore shipping areas	Far offshore locations within the designated shipping routes that fall within roughly 10 km from the boundaries of OWF's	575
Anchor zones	Offshore locations that fall within designated anchor zones within roughly 10 km from the boundaries of OWF's	20
Approach areas	Offshore locations that fall within designated approach areas within roughly 10 km from the boundaries of OWF's	56

The results presented here account for additional dependencies compared to the ones treated in the previous analysis report (Deltares, 2024). Next to directional dependencies concerning MWD and Dir U10 (North, East, South, West) and dependencies with various Hs and Tm-10 (Hs < 5 m, Hs > 5 m, Tm-10 < 10 s, Tm-10 > 10 s), in this report we update the results with the additional dependencies concerning wind speed classes (U10 < 10 m/s, U10 > 10 m/s) and atmospheric stability (unstable, neutral, stable atmosphere).

[2] N = sample size, Bias= mean(y)-mean(x), RMSE= root mean square error, std = Standard Deviation of error.

[3] Wakes can extend for more than 10 km from the OWF boundaries, however the effects are low and this is roughly the distance from which the wake effects become insignificant in terms of wave conditions. In addition, based on a sensitivity analysis of the buffer area (on a buffer distance of 5 km) it was observed that there is only a negligible difference in determined statistical parameters in comparison with those presented in the following sections for distances of less than 10 km.

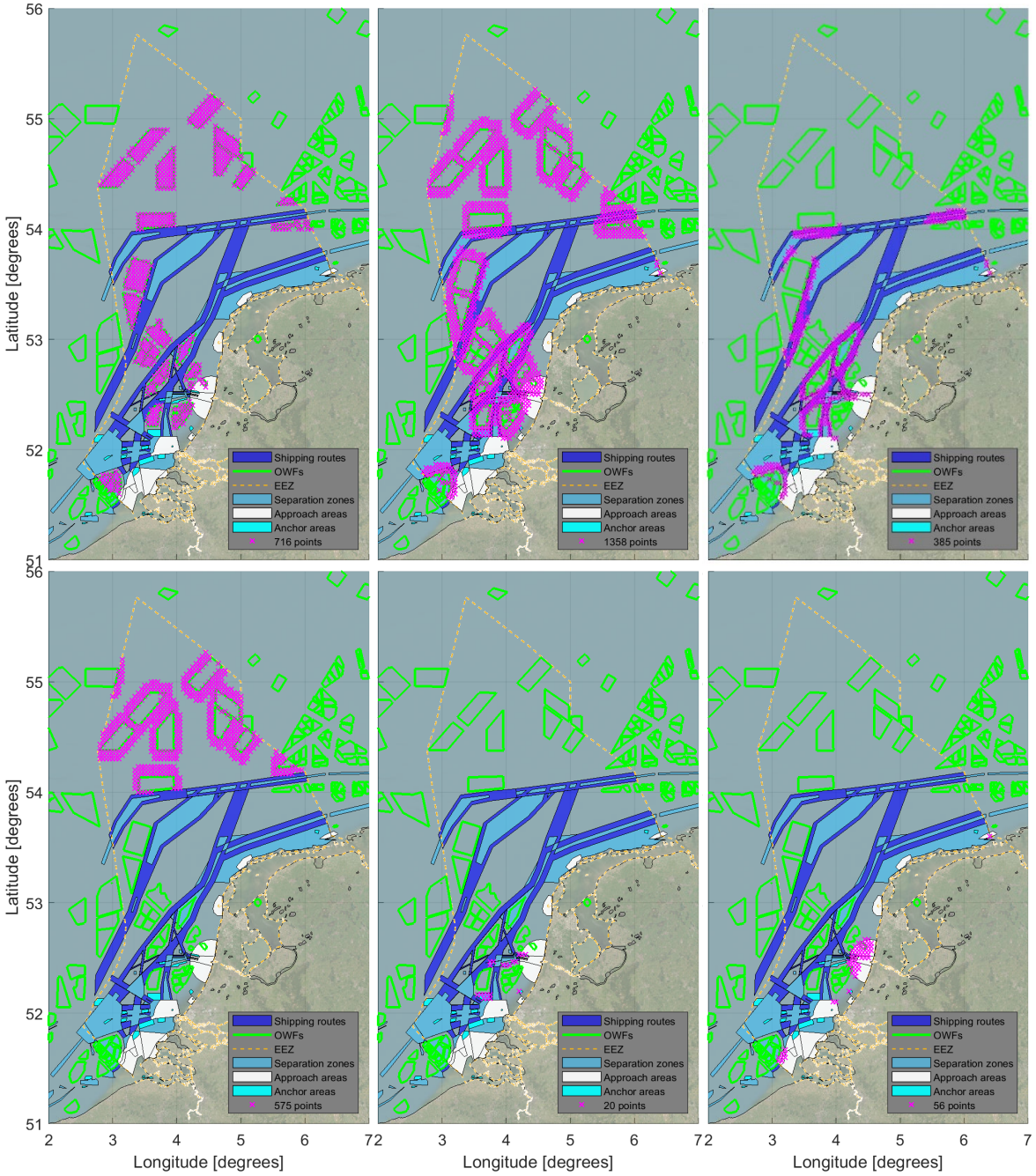

Figure 5.1 Clusters of relevant offshore locations within the Dutch EEZ, indicated by pink markers. Top: Dutch OWF (left), Surrounding area OWF (middle), Designated shipping routes (right), Bottom: Far offshore shipping areas (left), Anchor zones (middle panel), Approach areas (right panel).

5.2 Dutch 2050 OWF's

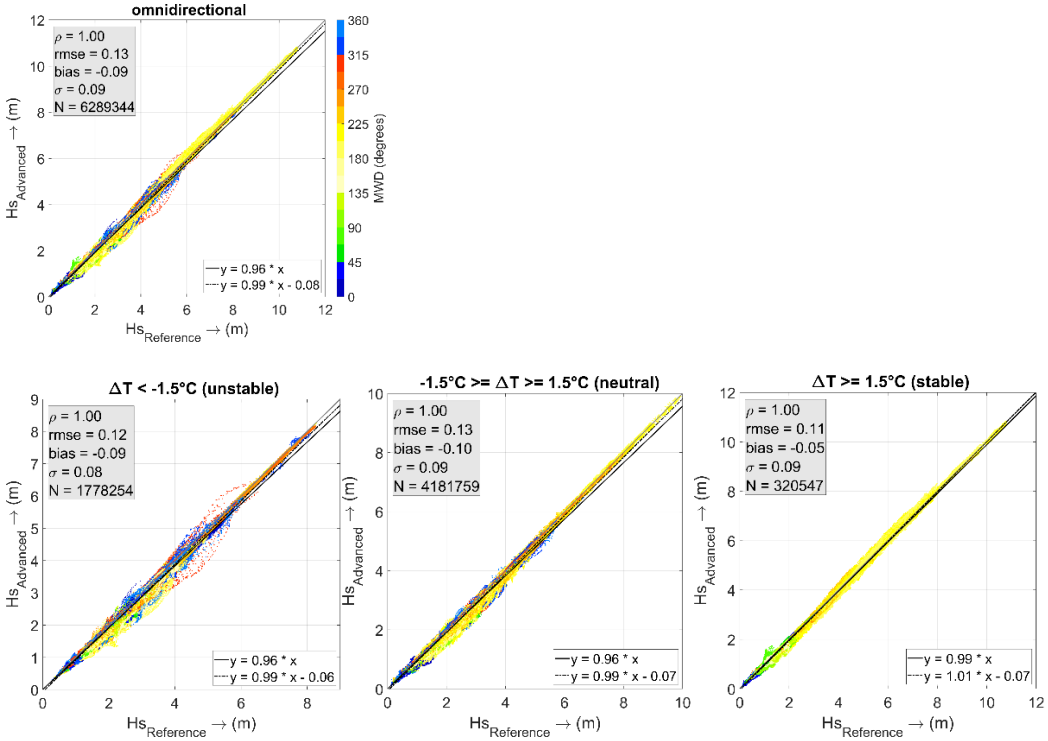

Figure 5.2 Scatter plot comparisons of significant wave height between Reference (x-axis) and Advanced (y-axis) wind schematization model results (simulation period from 01-2020 to 12-2020).

Table 5.2 Linear statistics of significant wave height (Hs) for the "Dutch 2050 OWF's" cluster (Advanced vs Reference) for various offshore conditions based on the full year 2020.

Condition	N [-]	Bias [m]	RMSE [m]	Symmetric Slope: (Adv) = a * (Ref) [-]	(Adv) = b * (Ref) + c	
					b [-]	c [-]
Omnidirectional	6289344	-0.09	0.13	0.96	0.99	-0.08
North MWD	2065464	-0.06	0.09	0.96	0.98	-0.03
Dir. U10 North	1084502	-0.08	0.11	0.96	0.98	-0.04
East MWD	642027	-0.09	0.12	0.93	0.96	-0.03
Dir. U10 East	1015075	-0.07	0.10	0.94	0.96	-0.01
South MWD	1418571	-0.13	0.17	0.96	1.01	-0.15
Dir. U10 South	1980443	-0.11	0.15	0.96	1.00	-0.10
West MWD	2163282	-0.10	0.13	0.96	0.99	-0.08
Dir. U10 West	2210963	-0.09	0.12	0.96	0.99	-0.07
Hs < 5 m	6138148	-0.09	0.13	0.95	0.98	-0.05
Hs > 5 m	151196	-0.05	0.10	0.99	1.02	-0.18
Tm-10 < 10 s	6249867	-0.09	0.13	0.96	0.99	-0.07
Tm-10 > 10 s	39477	-0.03	0.07	1.00	1.00	-0.04
U10 < 10 m/s	4160052	-0.06	0.09	0.95	0.98	-0.03
U10 > 10 m/s	2120508	-0.14	0.18	0.96	1.03	-0.22
Unstable atm.	1778254	-0.09	0.12	0.96	0.99	-0.06
Neutral atm.	4181759	-0.1	0.13	0.96	0.99	-0.07
Stable atm.	320547	-0.05	0.11	0.99	1.01	-0.07

Table 5.3 Linear statistics of mean absolute wave period (Tm-10) for the "Dutch 2050 OWF's" cluster (Advanced vs Reference) for various offshore conditions.

Condition	N [-]	Bias [s]	RMSE [s]	Symmetric Slope: (Adv) = a * (Ref) [-]	(Adv) = b*(Ref) +c	
					b [-]	c [-]
Omnidirectional	6289344	0.01	0.14	1.00	1.00	-0.01
North MWD	2065464	0.07	0.16	1.01	1.01	-0.01
Dir. U10 North	1084502	0.05	0.16	1.01	1.01	0.01
East MWD	642027	0.01	0.15	1.00	1.01	-0.04
Dir. U10 East	1015075	0.03	0.15	1.01	1.02	-0.05
South MWD	1418571	-0.06	0.14	0.99	1.00	-0.04
Dir. U10 South	1980443	-0.02	0.15	1.00	1.00	0.00
West MWD	2163282	0.01	0.13	1.00	1.00	0.03
Dir. U10 West	2210963	0.01	0.13	1.00	1.01	-0.04
Hs < 5 m	6138148	0.01	0.15	1.00	1.01	-0.05
Hs > 5 m	151196	-0.03	0.05	1.00	1.01	-0.15
Tm-10 < 10 s	6249867	0.01	0.14	1.00	1.01	-0.04
Tm-10 > 10 s	39477	0.01	0.08	1.00	0.98	0.27
U10 < 10 m/s	4160052	0.05	0.15	1.01	1.02	-0.07
U10 > 10 m/s	2120508	-0.06	0.13	0.99	1.02	-0.2
Unstable atm.	1778254	0.03	0.13	1.00	1.01	-0.01
Neutral atm.	4181759	0.01	0.15	1.00	1.00	-0.01
Stable atm.	320547	-0.03	0.13	0.99	1.00	-0.02

Table 5.4 Linear statistics of mean wave direction (MWD) for the "Dutch 2050 OWF's" cluster (Advanced vs Reference) for various offshore conditions.

Condition	N [-]	Bias [deg]	RMSE [deg]	std [deg]
Omnidirectional	6289344	-0.17	7.62	4.26
North MWD	2065464	-0.89	4.90	2.83
Dir. U10 North	1084502	-1.15	4.08	2.50
East MWD	642027	-4.35	11.86	4.63
Dir. U10 East	1015075	-2.77	8.37	4.22
South MWD	1418571	0.17	9.58	3.03
Dir. U10 South	1980443	0.99	10.73	3.81
West MWD	2163282	1.52	6.62	3.25
Dir. U10 West	2210963	0.46	4.66	2.76
Hs < 5 m	6138148	-0.18	7.71	4.31
Hs > 5 m	151196	0.09	0.53	0.52
Tm-10 < 10 s	6249867	-0.18	7.64	4.28
Tm-10 > 10 s	39477	0.15	0.69	0.68
U10 < 10 m/s	4160052	-0.2	8.84	3.83
U10 > 10 m/s	2120508	-0.13	4.31	2.49
Unstable atm.	1778254	-0.46	7.36	3.17
Neutral atm.	4181759	-0.07	7.73	4.60
Stable atm.	320547	0.03	7.62	3.52

5.3 Surrounding area Dutch OWF's

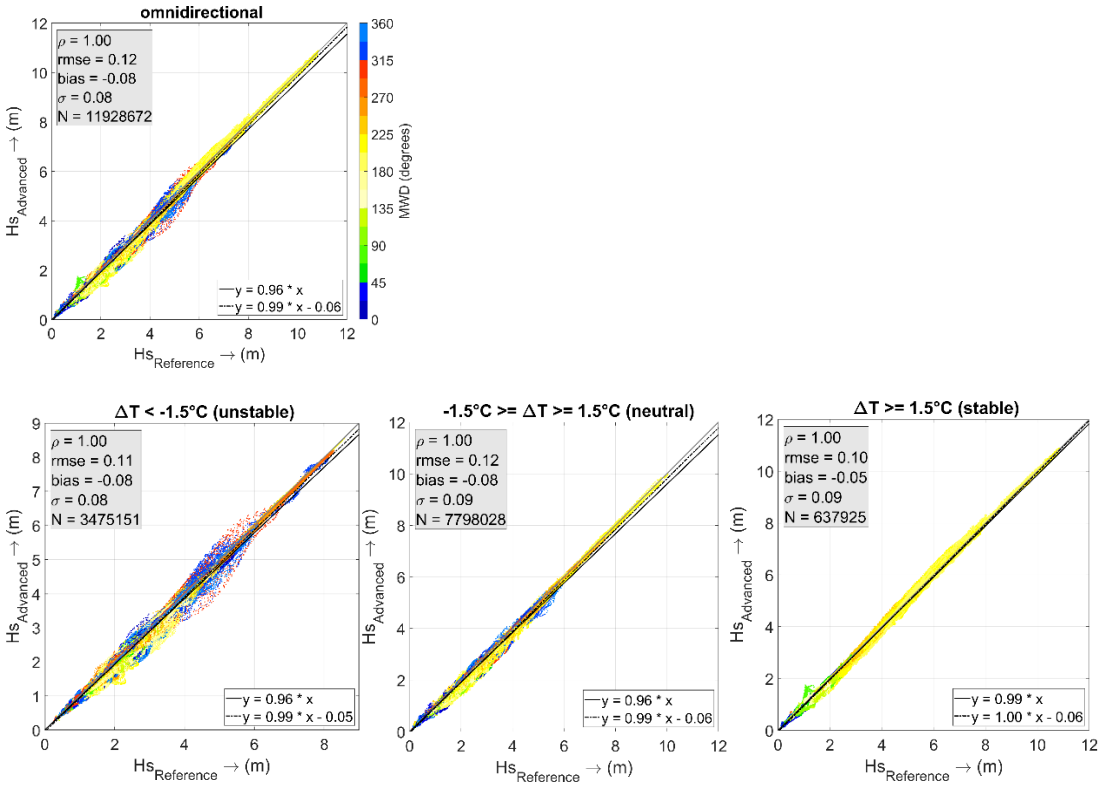

Figure 5.3 Scatter plot comparisons of significant wave height between Reference (x-axis) and Advanced (y-axis) wind schematization model results (simulation period from 01-2020 to 12-2020).

Table 5.5 Comparison statistics of significant wave height (Hs) for the "Surrounding area Dutch OWF's" cluster (Advanced vs Reference) for various offshore conditions.

Condition	N [-]	Bias [m]	RMSE [m]	Symmetric Slope: (Adv) = a * (Ref) [-]	(Adv) = b * (Ref) + c	
					b [-]	c [-]
Omnidirectional	11928672	-0.08	0.12	0.96	0.99	-0.06
North MWD	3936776	-0.05	0.08	0.97	0.97	-0.01
East MWD	1171863	-0.08	0.12	0.94	0.96	-0.03
South MWD	2572421	-0.12	0.16	0.96	1.00	-0.13
West MWD	4247612	-0.09	0.12	0.97	0.99	-0.07
Hs < 5 m	11659624	-0.08	0.12	0.96	0.98	-0.04
Hs > 5 m	269048	-0.05	0.10	0.99	1.02	-0.15
Tm-10 < 10 s	11861929	-0.08	0.12	0.96	0.99	-0.06
Tm-10 > 10 s	66743	-0.03	0.08	1.00	1.00	-0.03
U10 < 10 m/s	7880523	-0.06	0.08	0.96	0.98	-0.03
U10 > 10 m/s	4030581	-0.13	0.17	0.96	1.02	-0.190
Unstable atm.	3475151	-0.08	0.11	0.96	0.99	-0.05
Neutral atm.	7798028	-0.08	0.12	0.96	0.99	-0.06
Stable atm.	637925	-0.05	0.10	0.99	1.00	-0.06

5.4 Shipping routes within a buffer of 10km around OWF's

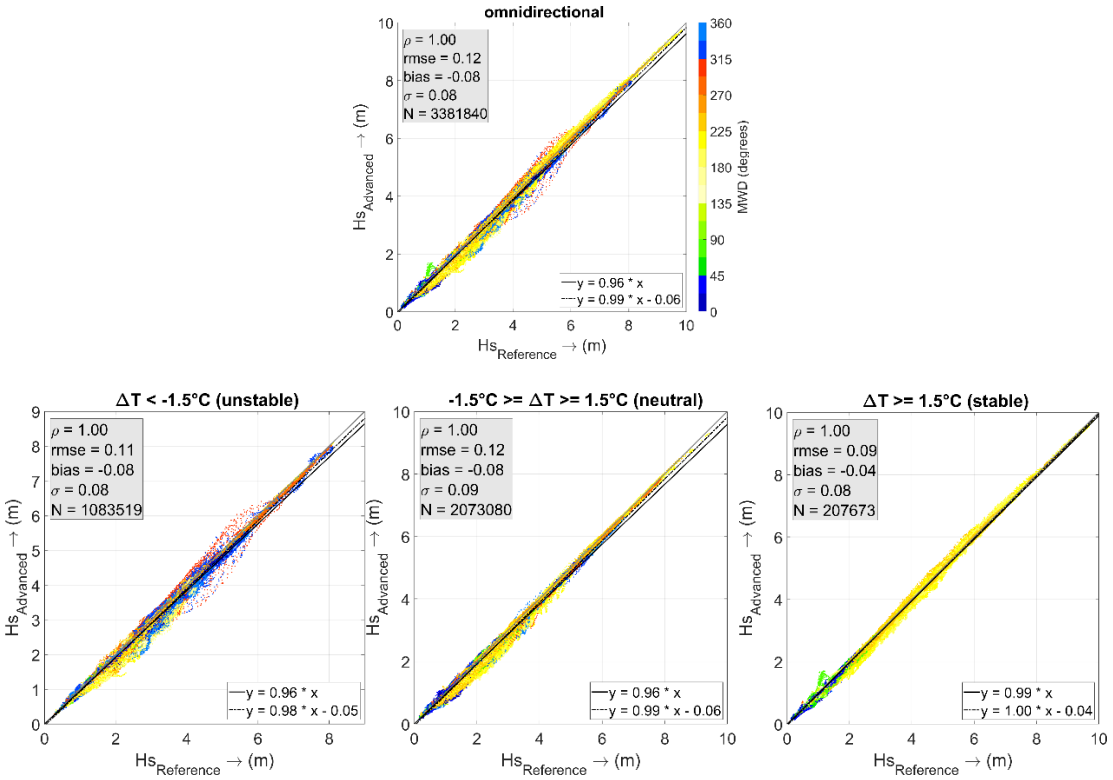

Figure 5.4 Scatter plot comparisons of significant wave height between Reference (x-axis) and Advanced (y-axis) wind schematization model results (simulation period from 01-2020 to 12-2020).

Table 5.6 Linear statistics of significant wave height (Hs) for the "Shipping routes within a buffer of 10km around OWF'sOWF's" cluster (Advanced vs Reference) for various offshore conditions.

Condition	N [-]	Bias [m]	RMSE [m]	Symmetric Slope: (Adv) = a * (Ref) [-]	(Adv) = b * (Ref) + c	
					b [-]	c [-]
Omnidirectional	3381840	-0.08	0.12	0.96	0.99	-0.06
North MWD	1158228	-0.05	0.08	0.96	0.98	-0.02
East MWD	290971	-0.05	0.09	0.96	0.97	-0.02
South MWD	694982	-0.12	0.16	0.96	1.00	-0.13
West MWD	1237659	-0.09	0.12	0.97	0.99	-0.07
Hs < 5 m	3323201	-0.08	0.12	0.96	0.98	-0.04
Hs > 5 m	58639	-0.04	0.09	0.99	1.01	-0.09
Tm-10 < 10 s	3373975	-0.08	0.12	0.96	0.99	-0.06
Tm-10 > 10 s	7865	-0.02	0.09	1.00	1.00	0.01
U10 < 10 m/s	2210162	-0.05	0.08	0.95	0.97	-0.02
U10 > 10 m/s	1154110	-0.130	0.16	0.96	1.02	-0.190
Unstable atm.	1083519	-0.08	0.11	0.96	0.98	-0.05
Neutral atm.	2073080	-0.08	0.12	0.96	0.99	-0.06
Stable atm.	207673	-0.04	0.09	0.99	1.00	-0.04

5.5 Far offshore within a buffer of 10km around OWF's

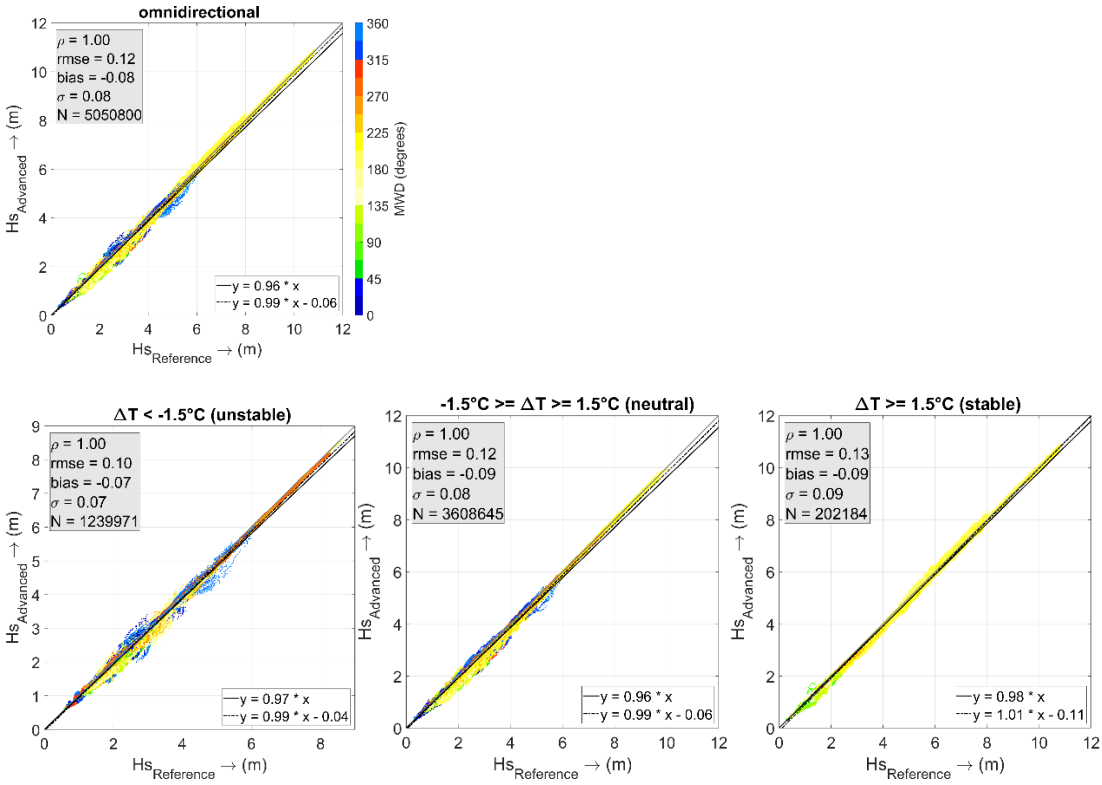

Figure 5.5 Scatter plot comparisons of significant wave height between Reference (x-axis) and Advanced (y-axis) wind schematization model results (simulation period from 01-2020 to 12-2020).

Table 5.7 Linear statistics of significant wave height (Hs) for the "Far offshore within a buffer of 10km around OWF'sOWF's" cluster (Advanced vs Reference) for various offshore conditions. N = sample size, Bias= mean(y)-mean(x), RMSE= root mean square error.

Condition	N [-]	Bias [m]	RMSE [m]	Symmetric Slope: (Adv) = a * (Ref) [-]	(Adv) = b * (Ref) + c	
					b [-]	c [-]
Omnidirectional	5050800	-0.08	0.12	0.96	0.99	-0.06
North MWD	1592164	-0.05	0.07	0.97	0.98	-0.02
East MWD	584058	-0.10	0.13	0.93	0.96	-0.04
South MWD	1198536	-0.12	0.15	0.96	1.00	-0.12
West MWD	1676042	-0.09	0.12	0.97	0.99	-0.06
Hs < 5 m	4895843	-0.08	0.12	0.96	0.97	-0.03
Hs > 5 m	154957	-0.07	0.10	0.99	1.02	-0.18
Tm-10 < 10 s	4999680	-0.08	0.12	0.96	0.99	-0.06
Tm-10 > 10 s	51120	-0.04	0.07	0.99	1.00	-0.04
U10 < 10 m/s	3357949	-0.06	0.08	0.96	0.98	-0.03
U10 > 10 m/s	1692851	-0.140	0.17	0.97	1.02	-0.2
Unstable atm.	1239971	-0.07	0.1	0.97	0.99	-0.04
Neutral atm.	3608645	-0.09	0.12	0.96	0.99	-0.06
Stable atm.	202184	-0.09	0.13	0.98	1.01	-0.11

5.6 Anchor zones

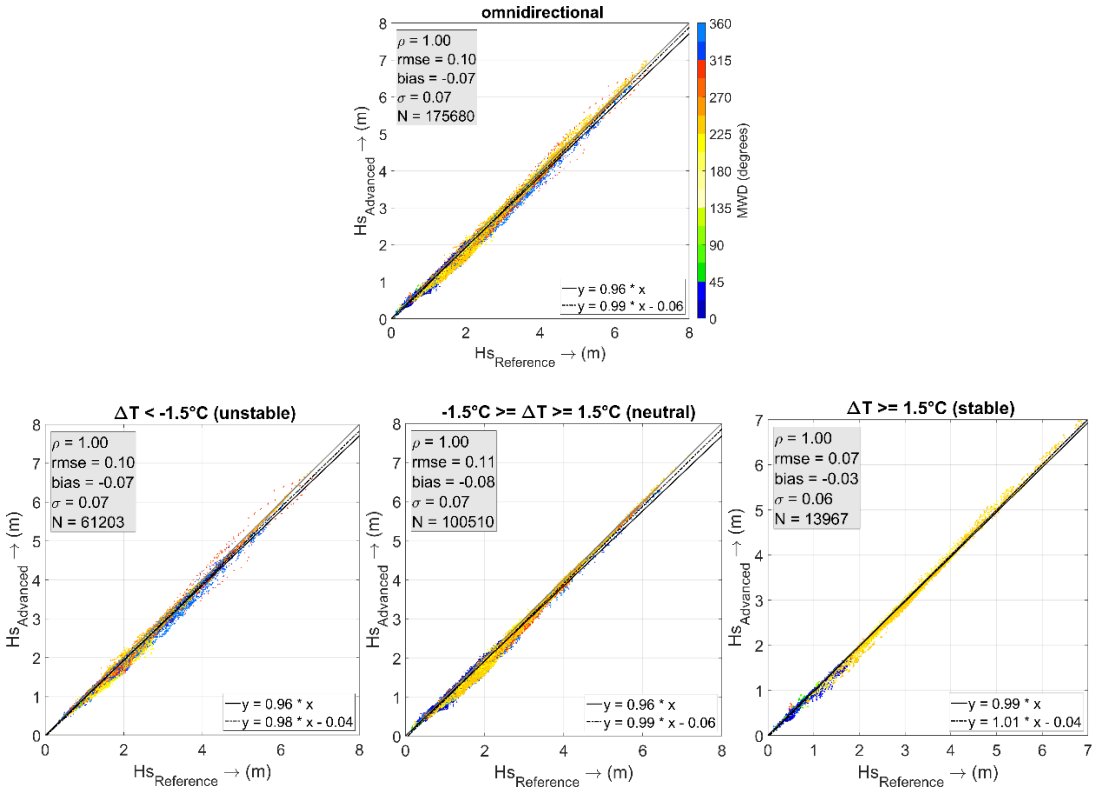

Figure 5.6 Scatter plot comparisons of significant wave height between Reference (x-axis) and Advanced (y-axis) wind schematization model results (simulation period from 01-2020 to 12-2020).

Table 5.8 Linear statistics of significant wave height (Hs) for the "Anchor zonesOWF's" cluster (Advanced vs Reference) for various offshore conditions. N = sample size, Bias= mean(y)-mean(x), RMSE= root mean square error.

Condition	N [-]	Bias [m]	RMSE [m]	Symmetric Slope: (Adv) = a * (Ref) [-]	(Adv) = b * (Ref) + c	
					b [-]	c [-]
Omnidirectional	175680	-0.07	0.10	0.96	0.99	-0.06
North MWD	62639	-0.05	0.09	0.96	0.97	-0.01
East MWD	8965	-0.04	0.06	0.96	0.95	0.01
South MWD	25280	-0.09	0.12	0.96	1.00	-0.10
West MWD	78796	-0.08	0.11	0.97	1.00	-0.08
Hs < 5 m	173521	-0.07	0.10	0.96	0.98	-0.04
Hs > 5 m	2159	-0.03	0.09	0.99	1.04	-0.26
Tm-10 < 10 s	175600	-0.07	0.10	0.96	0.99	-0.06
Tm-10 > 10 s	0	-	-	-	-	-
U10 < 10 m/s	114865	-0.05	0.08	0.95	0.970	-0.02
U10 > 10 m/s	60815	-0.110	0.14	0.97	1.03	-0.17
Unstable atm.	61203	-0.07	0.10	0.96	0.98	-0.04
Neutral atm.	100510	-0.08	0.11	0.96	0.99	-0.06
Stable atm.	13967	-0.03	0.07	0.99	1.01	-0.04

5.7 Approach areas

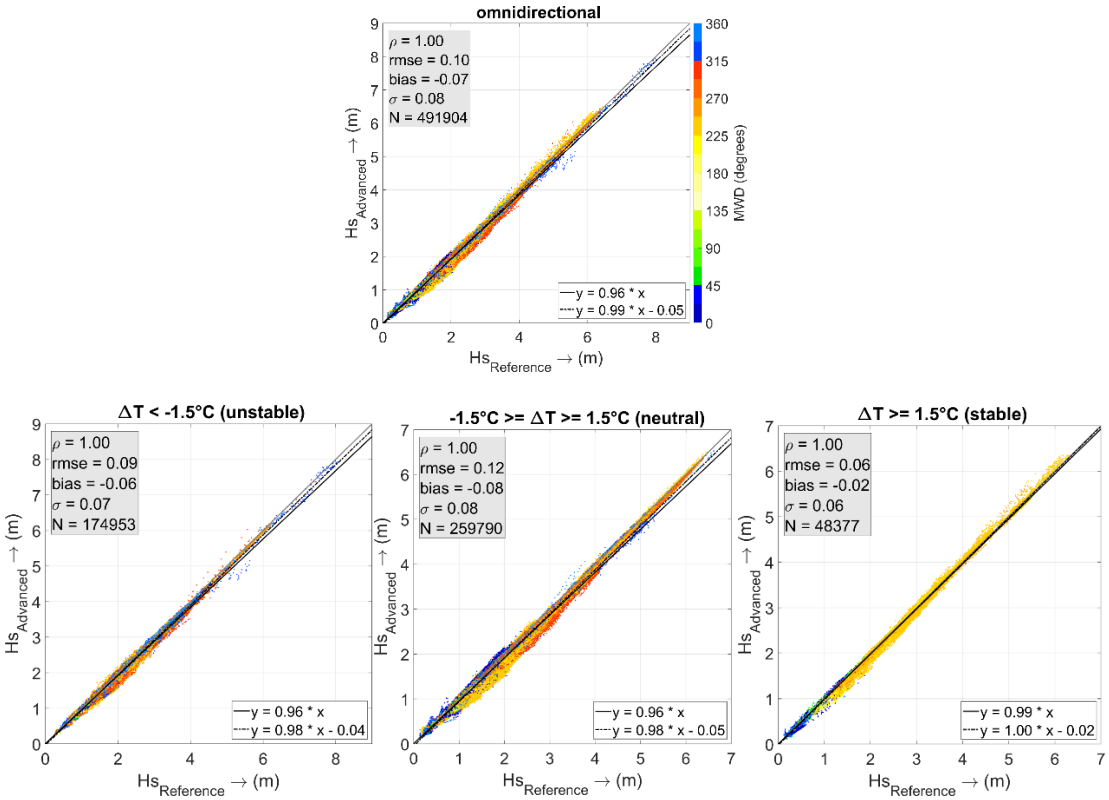

Figure 5.7 Scatter plot comparisons of significant wave height between Reference (x-axis) and Advanced (y-axis) wind schematization model results (simulation period from 01-2020 to 12-2020).

Table 5.9 Linear statistics of significant wave height (Hs) for the "Approach areasOWF's" cluster (Advanced vs Reference) for various offshore conditions. N = sample size, Bias= mean(y)-mean(x), RMSE= root mean square error.

Condition	N [-]	Bias [m]	RMSE [m]	Symmetric Slope: (Adv) = a * (Ref) [-]	(Adv) = b * (Ref) + c	
					b [-]	c [-]
Omnidirectional	491904	-0.07	0.10	0.96	0.99	-0.05
North MWD	170847	-0.03	0.06	0.97	0.99	-0.01
East MWD	19658	-0.02	0.03	0.98	0.98	0.00
South MWD	49840	-0.06	0.08	0.96	0.99	-0.05
West MWD	251559	-0.10	0.13	0.96	1.00	-0.09
Hs < 5 m	487281	-0.07	0.10	0.96	0.98	-0.03
Hs > 5 m	4623	-0.03	0.08	0.99	1.01	-0.10
Tm-10 < 10 s	491355	-0.07	0.10	0.96	0.98	-0.04
Tm-10 > 10 s	549	-0.02	0.07	0.99	0.99	0.03
U10 < 10 m/s	330712	-0.05	0.08	0.95	0.96	0
U10 > 10 m/s	152408	-0.11	0.14	0.96	1.02	-0.15
Unstable atm.	174953	-0.06	0.09	0.96	0.98	-0.04
Neutral atm.	259790	-0.08	0.12	0.96	0.98	-0.05
Stable atm.	48377	-0.02	0.06	0.99	1.00	-0.02

5.8 Discussion

In this section, the results of the statistical analysis are compiled per cluster for the complete dataset (no filtering - omnidirectional) as well as for the various additional dependencies considered in this phase of the project, concerning significant wave weight in specific, which is the wave integral parameter influenced predominantly by the operation of the wind farms, as opposed to wave period and propagation direction, at least according to the simulation results (see e.g., Table 5.3).

Table 5.10 Omnidirectional statistics of Hs (Reference versus Advanced wind schematization). Bias defined as Y-X so a positive bias implies increased wave heights due to the OWF and vice versa.

Cluster	N [-]	Bias [m]	RMSE [m]	Symetric Slope: (Adv) = a * (Ref) [-]	(Adv) = b * (Ref) + c	
					b [-]	c [-]
Dutch OWF's	6289344	-0.09	0.13	0.96	0.99	-0.08
Surrounding OWF's	11928672	-0.08	0.12	0.96	0.99	-0.06
Shipping routes	3381840	-0.08	0.12	0.96	0.99	-0.06
Far offshore shipping routes	5050800	-0.08	0.12	0.96	0.99	-0.06
Anchor zones	175680	-0.07	0.10	0.96	0.99	-0.06
Approach areas	491904	-0.07	0.10	0.96	0.99	-0.05

Table 5.11 Omnidirectional statistics of Hs (Reference versus Advanced wind schematization) for U10 < 10 m/s.

Cluster	N [-]	Bias [m]	RMSE [m]	Symetric Slope: (Adv) = a * (Ref) [-]	(Adv) = b * (Ref) + c	
					b [-]	c [-]
Dutch OWF's	4160052	-0.06	0.09	0.95	0.98	-0.03
Surrounding OWF's	7880523	-0.06	0.08	0.96	0.98	-0.03
Shipping routes	2210162	-0.05	0.08	0.95	0.97	-0.02
Far offshore shipping routes	3357949	-0.06	0.08	0.96	0.98	-0.03
Anchor zones	114865	-0.05	0.08	0.95	0.97	-0.02
Approach areas	330712	-0.05	0.08	0.95	0.96	0

Table 5.12 Omnidirectional statistics of Hs (Reference versus Advanced wind schematization) for U10 > 10 m/s.

Cluster	N [-]	Bias [m]	RMSE [m]	Symetric Slope: (Adv) = a * (Ref) [-]	(Adv) = b * (Ref) + c	
					b [-]	c [-]
Dutch OWF's	2120508	-0.14	0.18	0.96	1.03	-0.22
Surrounding OWF's	4030581	-0.13	0.17	0.96	1.02	-0.19
Shipping routes	1154110	-0.13	0.16	0.96	1.02	-0.19
Far offshore shipping routes	1692851	-0.14	0.17	0.97	1.02	-0.2
Anchor zones	60815	-0.11	0.14	0.97	1.03	-0.17
Approach areas	152408	-0.11	0.14	0.96	1.02	-0.15

Table 5.13 Omnidirectional statistics of Hs (Reference versus Advanced wind schematization) for unstable atmosphere.

Cluster	N [-]	Bias [m]	RMSE [m]	Symetric Slope: (Adv) = a * (Ref) [-]	(Adv) = b * (Ref) + c	
					b [-]	c [-]
Dutch OWF's	1778254	-0.09	0.12	0.96	0.99	-0.06
Surrounding OWF's	3475151	-0.08	0.11	0.96	0.99	-0.05
Shipping routes	1083519	-0.08	0.11	0.96	0.98	-0.05
Far offshore shipping routes	1239971	-0.07	0.10	0.97	0.99	-0.04
Anchor zones	61203	-0.07	0.10	0.96	0.98	-0.04
Approach areas	174953	-0.06	0.09	0.96	0.98	-0.04

Table 5.14 Omnidirectional statistics of Hs (Reference versus Advanced wind schematization) for neutral atmosphere.

Cluster	N [-]	Bias [m]	RMSE [m]	Symetric Slope: (Adv) = a * (Ref) [-]	(Adv) = b * (Ref) + c	
					b [-]	c [-]
Dutch OWF's	4181759	-0.10	0.13	0.96	0.99	-0.07
Surrounding OWF's	7798028	-0.08	0.12	0.96	0.99	-0.06
Shipping routes	2073080	-0.08	0.12	0.96	0.99	-0.06
Far offshore shipping routes	3608645	-0.09	0.12	0.96	0.99	-0.06
Anchor zones	100510	-0.08	0.11	0.96	0.99	-0.06
Approach areas	259790	-0.08	0.12	0.96	0.98	-0.05

Table 5.15 Omnidirectional statistics of Hs (Reference versus Advanced wind schematization) for stable atmosphere.

Cluster	N [-]	Bias [m]	RMSE [m]	Symetric Slope: (Adv) = a * (Ref) [-]	(Adv) = b * (Ref) + c	
					b [-]	c [-]
Dutch OWF's	320547	-0.05	0.11	0.99	1.01	-0.07
Surrounding OWF's	637925	-0.05	0.10	0.99	1.00	-0.06
Shipping routes	207673	-0.04	0.09	0.99	1.00	-0.04
Far offshore shipping routes	202184	-0.09	0.13	0.98	1.01	-0.11
Anchor zones	13967	-0.03	0.07	0.99	1.01	-0.04
Approach areas	48377	-0.02	0.06	0.99	1.00	-0.02

Observations

- As discussed in the previous phase of this project, waves appear to predominantly decrease as a result of the operation of offshore wind farms, when all conditions are considered (Table 5.10). This is due to extraction of wind and consequently reduction of wave generation in the vicinity of offshore wind farms. This decrease expressed in significant wave height is in the order of 4% compared to reference conditions (no OWF operation) within OWF's and across various areas of navigational interest in the vicinity of OWF's alike.

- For both considered wind speed classes assessed in the present statistical analysis, the reduction in Hs appears to be in a similar order of magnitude as in yearly round omnidirectional conditions (Table 5.10 and Table 5.11, Table 5.12). The decrease in Hs is slightly more pronounced in the case of U10 < 10 m/s compared to U10 > 10 m/s, based on the Symmetric Slope (SS) fit through the data. The difference in observed Hs reduction is nearly negligible between different considered areas with respect to navigational interest and OWF position.

- The Hs reduction varies between different atmospheric stability conditions (Table 5.10 and Table 5.13, Table 5.14, Table 5.15). For the most-frequently occurring in the North Sea unstable and neutral atmospheric conditions, the reduction in Hs is of the same order of magnitude as for the omnidirectional year-round conditions, i.e., ~4%. For the less frequently occurring stable atmosphere, the reduction in Hs due to OWF operation is nearly negligible. From the linear fit in e.g., Figure 5.2 (bottom right panel), it is also evident that the combination of stable atmosphere with a relatively energetic wave climate may lead to a slight amplification of wave energy as a result of OWF operation. This is due to the downward transfer of momentum by the rotating blades in these conditions.

6 Conclusions

6.1 Semi-advanced wind schematization

In this study, a semi-advanced schematization of OWF impacts on wind fields was developed, as a further advancement of the crude approximation involving a constant and uniform reduction if 10% in wind speeds only across offshore wind farms. With this semi-advanced approach – based on the WINS50 set - a fast and more realistic method of accounting for wind impacts from OWF operation is achieved by considering a condition dependent wind deficit across wind farms as well as the wake region downwind from the OWF polygon.

This allows for the simulation of OWF impacts on the atmosphere, waves and currents over a larger period of time (employing ERA5 hindcast datasets) compared to the WINS50 simulation and hence the assessment of more extreme and / or relevant events. At the same time, this semi-advanced approach allows for a representation of relevant physical processes related to wind with higher accuracy compared to the crude approximation employed previously. This method is not location or OWF specific, and may be applied at different regions of the world and for various alternative OWF scenarios.

The performance of the synthetic wind field generation may be evaluated in future steps of the study.

6.2 Currents

While OWF's do not impose sufficiently large effect on the current velocity in general, the instantaneous differences can reach up to 0.5 m/s compared to situation without wind farms. It was not proved, however, that these differences can pose immediate threat to the navigation safety as they are not occurring suddenly.

The strength of the effect was found to be lightly dependent on the meteorological factors such as wind speed, wind direction, or atmospheric stability. However, it should be noted that the variability of current velocity in the leeward side of wind parks in relation to the dominant wind directions (western winds) will grow with the growth of offshore infrastructure.

The strength of OWF's effect is more strongly affected by proximity to the wind park. According to the determined statistics the largest effect would be observed within OWF's themselves, which may have an influence on navigation safety for small-scale vessels travelling within wind parks.

6.3 Waves

In this phase of the study, the previous statistical analysis concerning changes in Hs, Tm-10 and MWD was extended with additional investigation of dependencies on wind speed and atmospheric conditions.

The previous observation concerning a significant wave height reduction as a result of OWF operation is also obtained for the additional dependencies considered. With respect to wind speeds, the Hs reduction is in the same order as the omnidirectional year-round condition (~4% reduction due to OWF operation). The same holds for the two most frequently occurring atmospheric conditions in the North Sea, i.e., unstable and neutral atmosphere. Only for the more rarely occurring (~roughly 5% of duration within assessment year) stable atmospheric conditions, the waves appear to not reduce as a result of the OWF operation. In fact, in certain

cases (stable atmosphere and relatively energetic wave climate), waves may be slightly amplified as a result of OWF operation.

There is limited variation of Hs reduction observed with respect to different areas of navigation interest assessed, i.e., the OWF effect is similar within and around OWF's, across approach channels, anchor areas as well as navigational routes further offshore.

References

Deltares, 2025: First Steps to Assess How Offshore Wind Farms Affect Waves and Currents dd 22 Jan 2025, ref 11210382-001-HYE-0001 (Offshore Wind Energy Shipping Safety Monitoring and Research Programme (MOSWOZ))

Cañadillas, B., Beckenbauer, M., Trujillo, J. J., Dörenkämper, M., Foreman, R., Neumann, T., and Lampert, A.: Offshore wind farm cluster wakes as observed by long-range-scanning wind lidar measurements and mesoscale modeling, Wind Energ. Sci., 7, 1241–1262, https://doi.org/10.5194/wes-7-1241-2022, 2022.

Fitch A.C., J. B. Olson, J. K. Lundquist, J. Dudhia, A. K. Gupta, J. Michalakes, and I. Barstad (2012). Monthly Weather Review, 140(9), pp. 3017-3038

Gautier, C. and S. Caires (2015). Operational wave forecasts in the southern North Sea, in 36th IAHR World Congress, 28 Jun – 3 Jul, p.5.

Hersbach, H., Bell, B., Berrisford, P., Hirahara, S., Horányi, A., Muñoz-Sabater, J. et al. (2020). The ERA5 global reanalysis. *Quarterly Journal of the Royal Meteorological Society*, **146**, 1999–2049. Available from: https://doi.org/10.1002/qj.3803

Zijl et al. (2021) Potential ecosystem effects of large upscaling of offshore wind in the North Sea; Bottom-up approach dd 22 April 2021. Deltares report 11203731-004-ZKS-0015.

Zijl, F., T. Zijlker, S. Laan and J. Groenenboom (2023). 3D DCSM-FM: a sixth-generation model for the NW European Shelf (2022 release). Deltares, report 11208054-004-ZKS-0003, Delft.

Zijl, F., L. Leummens, N. Alexandrova, T. Van Kessel, L. Jaksic, V. T. M. van Zelst, L. M. Vilmin, S. Heye, and L. A. Van Duren (2024). Impact of offshore wind farms on the North Sea ecosystem. Scenario study for the partial revision of the Dutch offshore wind planning. 11209248-006-ZKS-0001, Deltares, Delft.

Zijl, F. and L. Leummens (2024). The effect of wind wakes on hydrodynamic parameters. Deltares report 11209248-003-ZKS-0001.

A Full results: wind deficit and wake length

A.1 Median Wind Deficit within OWF

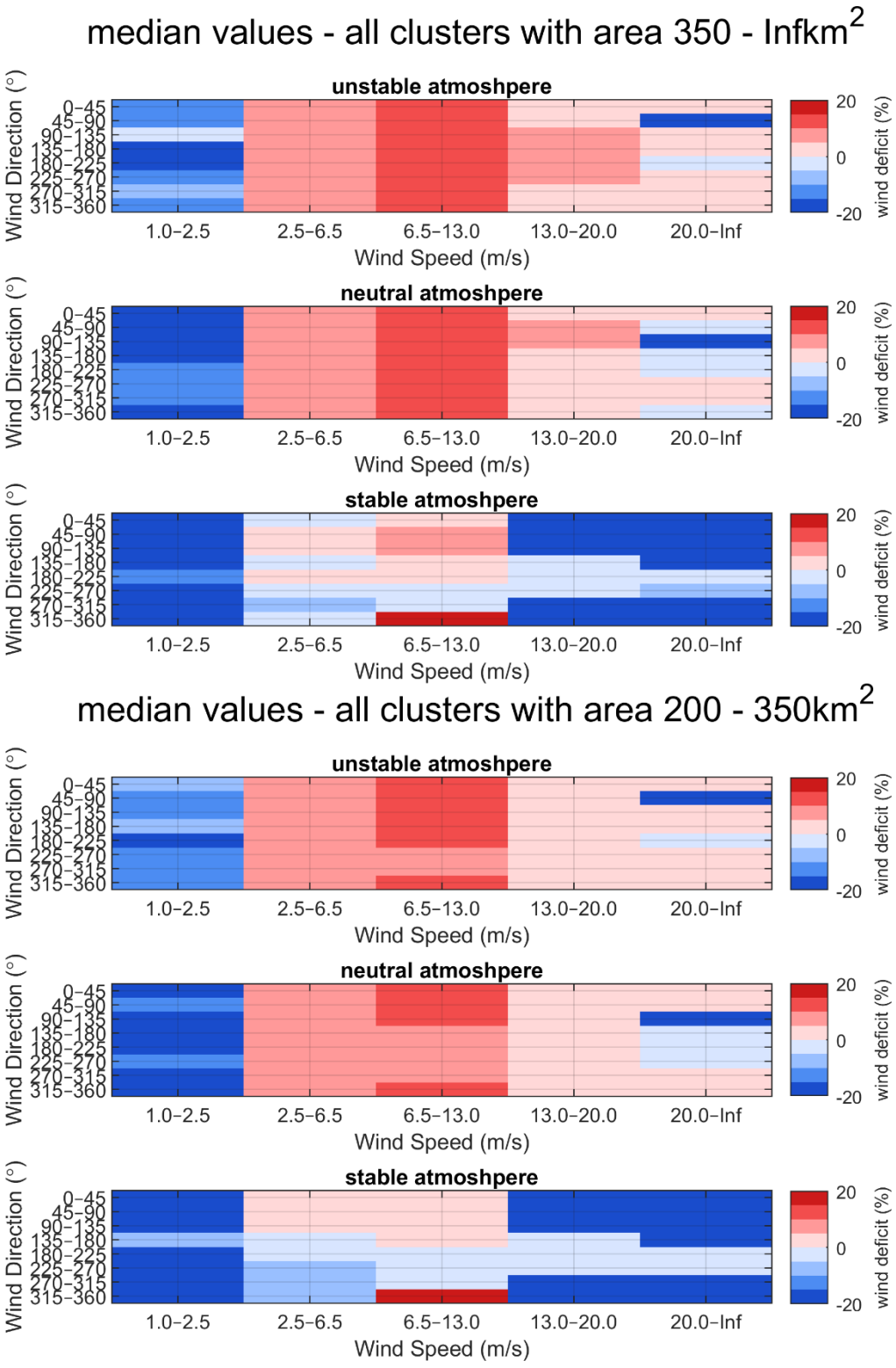

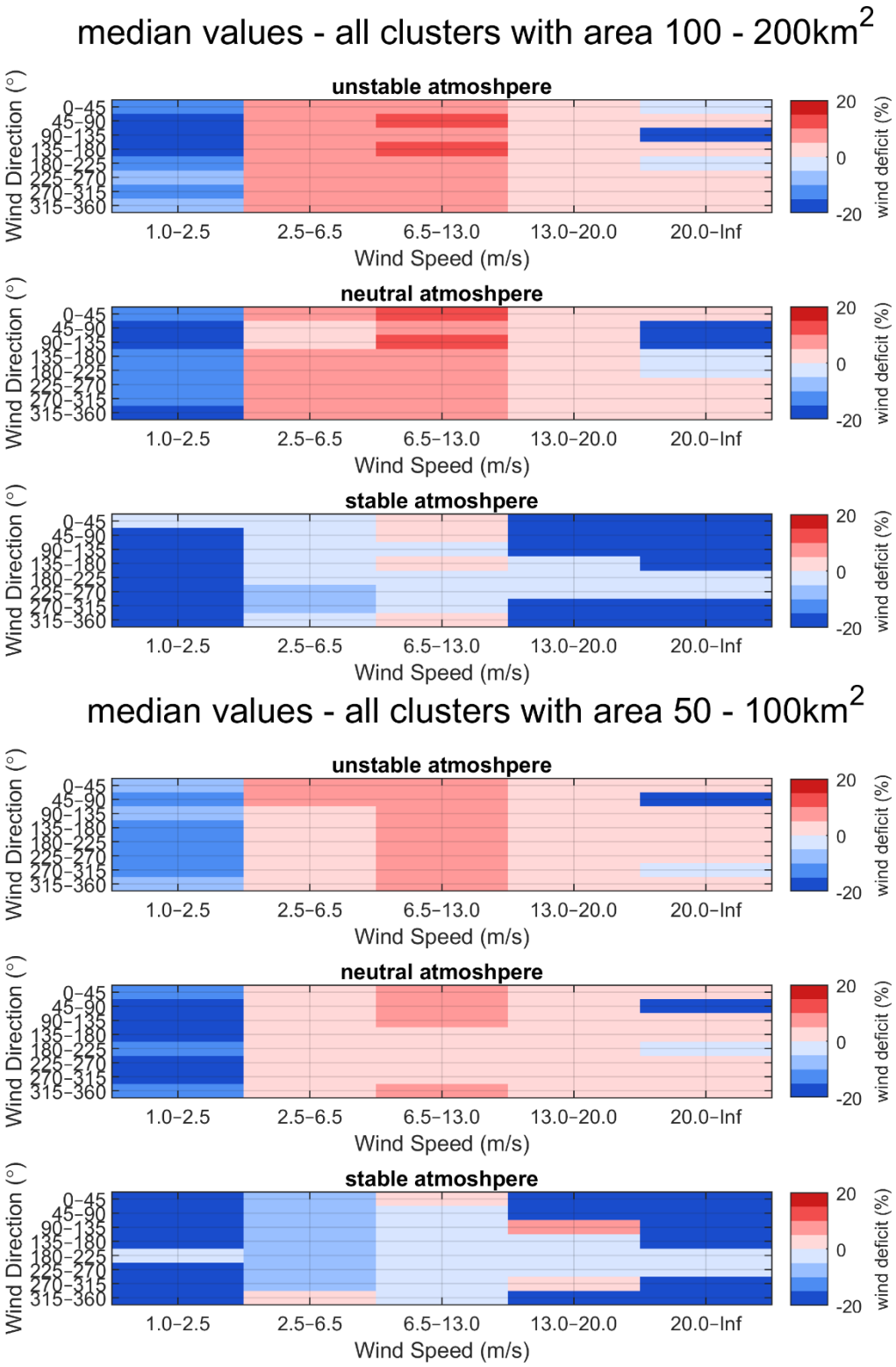
median values - all clusters with area 100 - 200km2
unstable atmoshpere
neutral atmoshpere
stable atmoshpere
median values - all clusters with area 50 - 100km2
unstable atmoshpere
neutral atmoshpere
stable atmoshpere
Wind Direction (°)
0-45
45-90
90-135
135-180
180-225
225-270
270-315
315-360
1.0-2.5
2.5-6.5
6.5-13.0
13.0-20.0
20.0-Inf
Wind Speed (m/s)
wind deficit (%)
20
0
-20

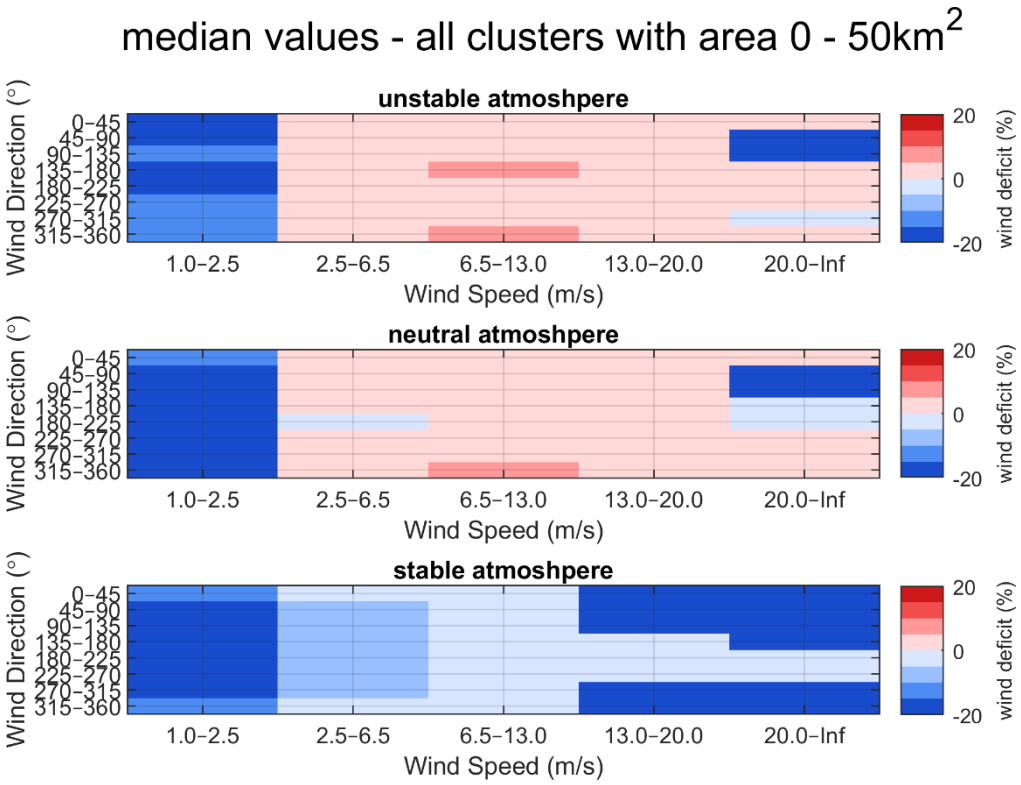
median values - all clusters with area 0 - 50km2
unstable atmoshpere
neutral atmoshpere
stable atmoshpere
Wind Direction (°)
0-45
45-90
90-135
135-180
180-225
225-270
270-315
315-360
1.0-2.5
2.5-6.5
6.5-13.0
13.0-20.0
20.0-Inf
Wind Speed (m/s)
20
0
-20
wind deficit (%)

A.2 Median Wake Length

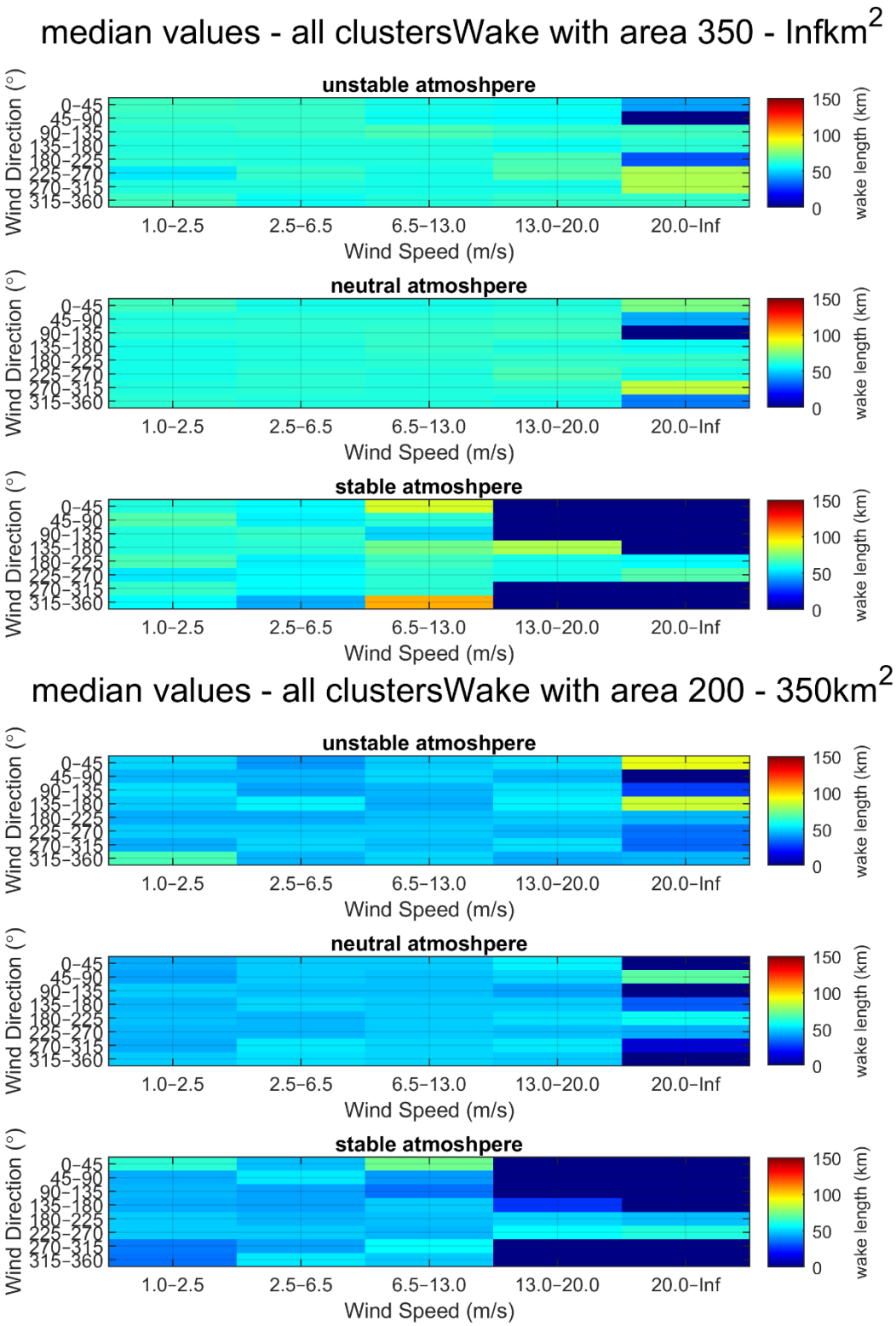

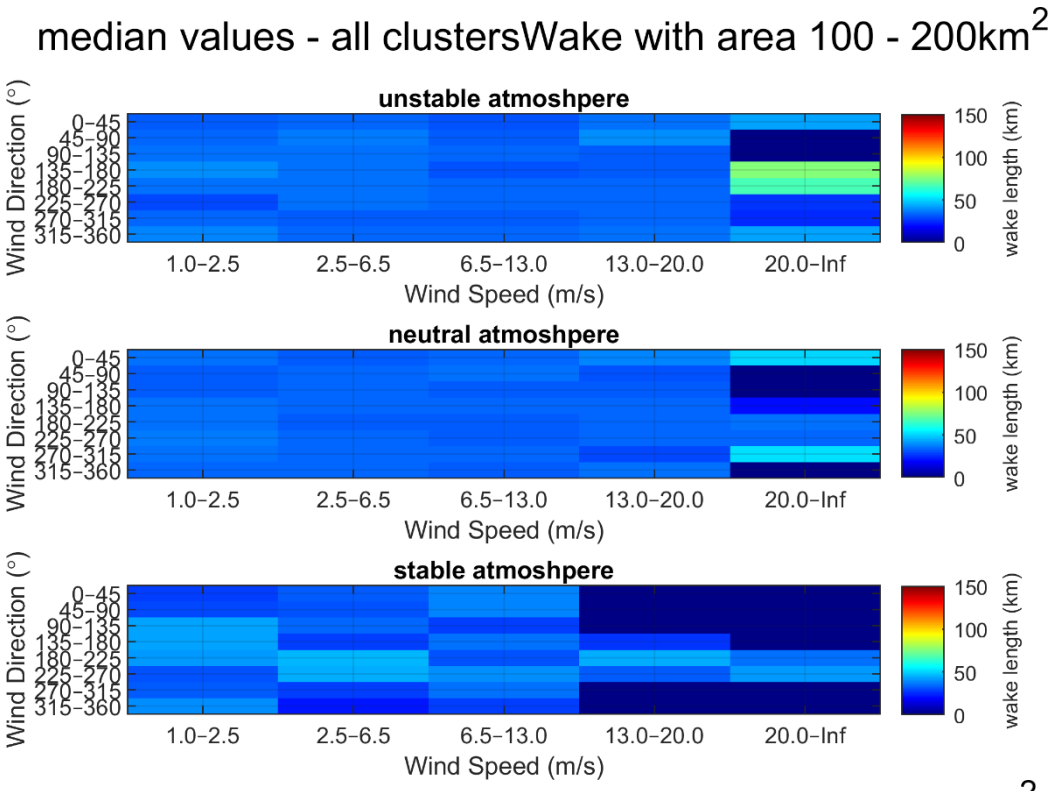
median values - all clustersWake with area 100 - 200km2
unstable atmoshpere
neutral atmoshpere
stable atmoshpere
Wind Direction (°)
0-45
45-90
90-135
135-180
180-225
225-270
270-315
315-360
1.0-2.5
2.5-6.5
6.5-13.0
13.0-20.0
20.0-Inf
Wind Speed (m/s)
wake length (km)
150
100
50
0

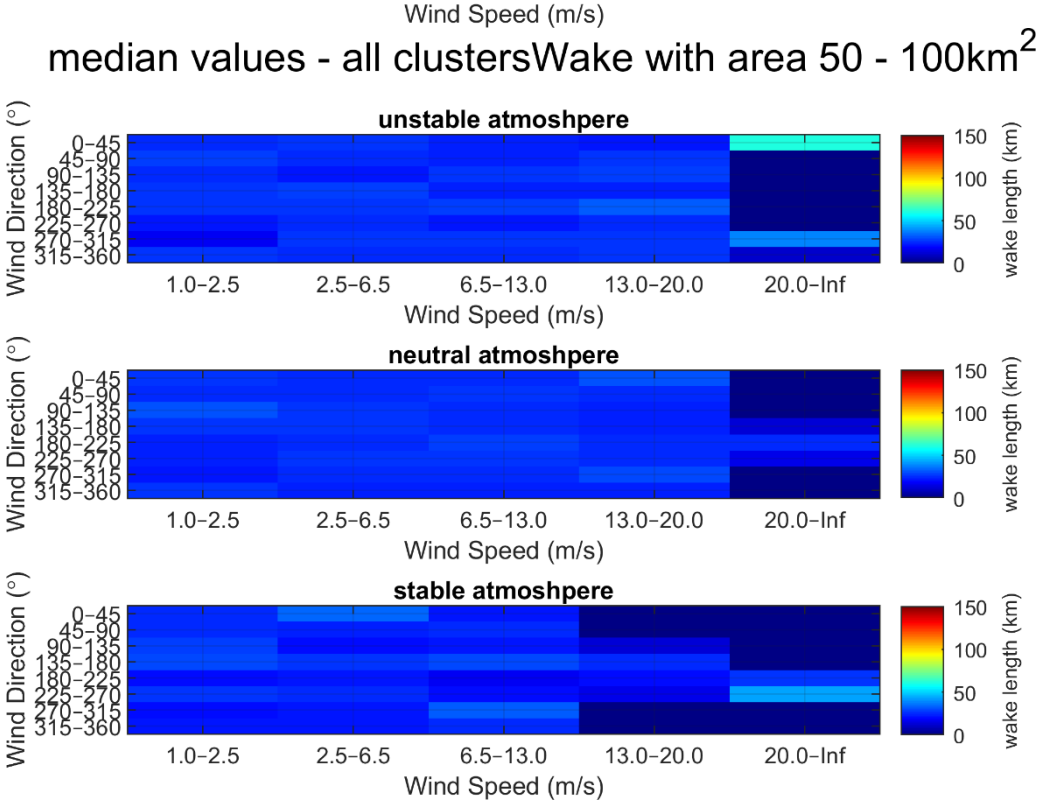
median values - all clustersWake with area 50 - 100km2
unstable atmoshpere
neutral atmoshpere
stable atmoshpere
Wind Direction (°)
0-45
45-90
90-135
135-180
180-225
225-270
270-315
315-360
1.0-2.5
2.5-6.5
6.5-13.0
13.0-20.0
20.0-Inf
Wind Speed (m/s)
wake length (km)
150
100
50
0

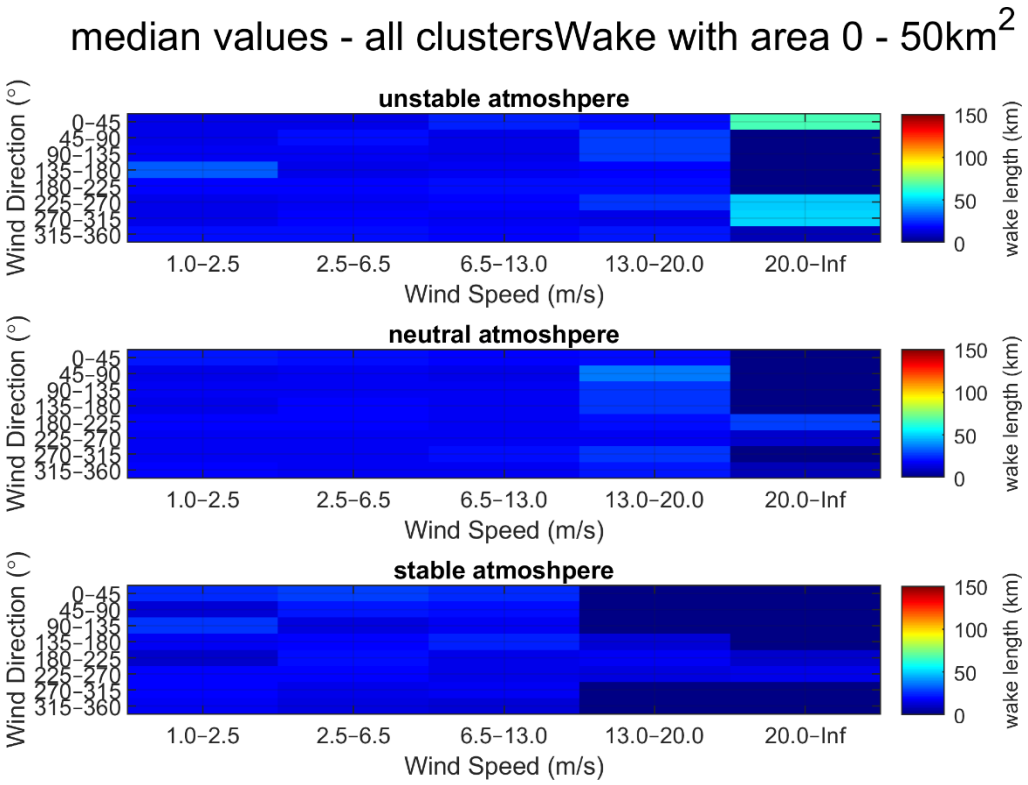

A.3 Median Wind Deficit within Wake Region

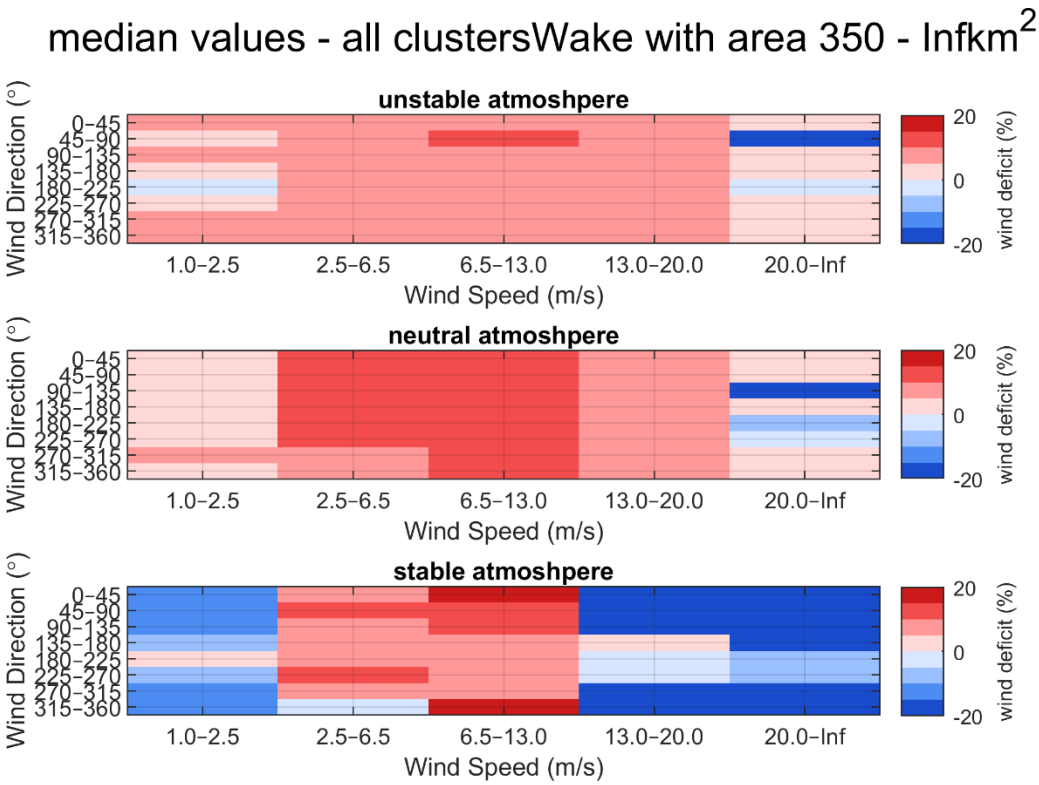

median values - all clustersWake with area 200 - 350km^2

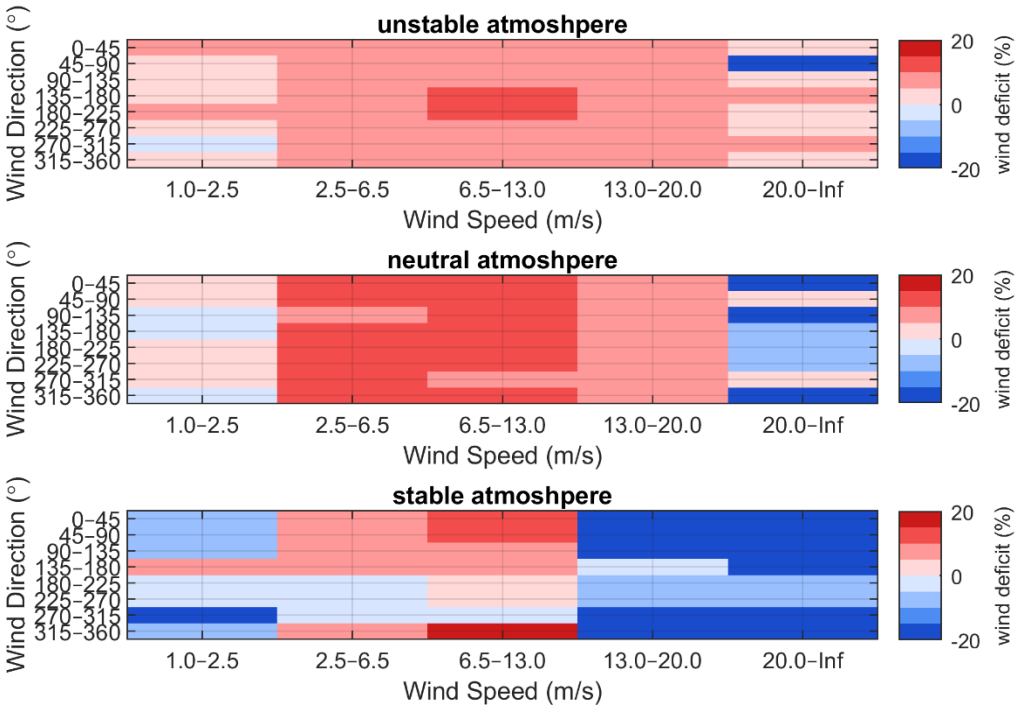

median values - all clustersWake with area 100 - 200km^2

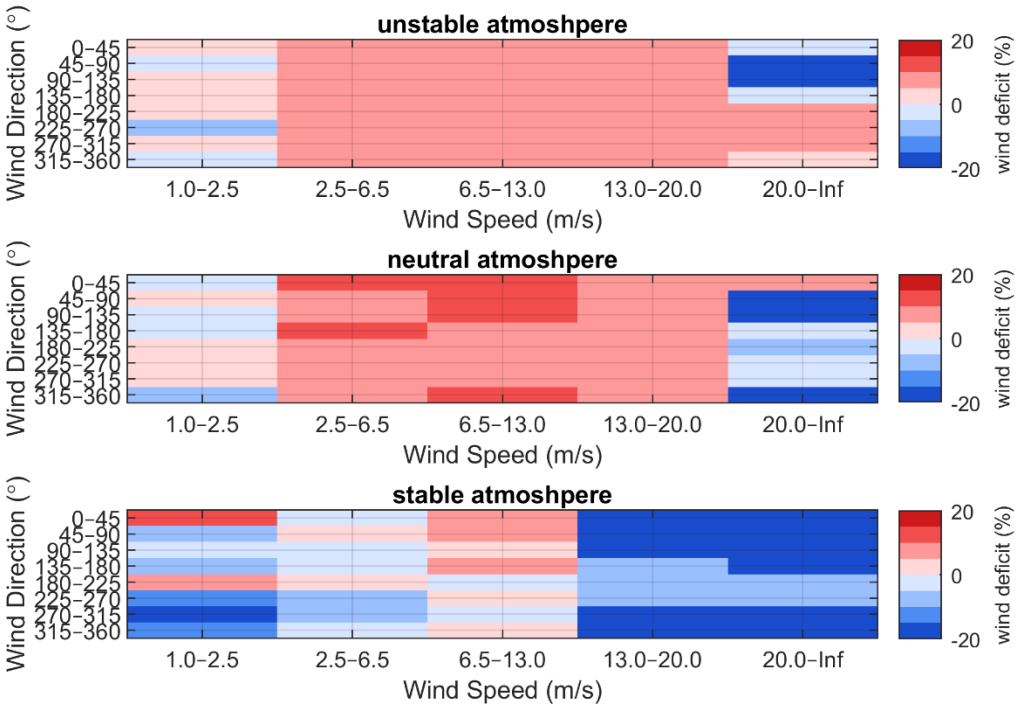

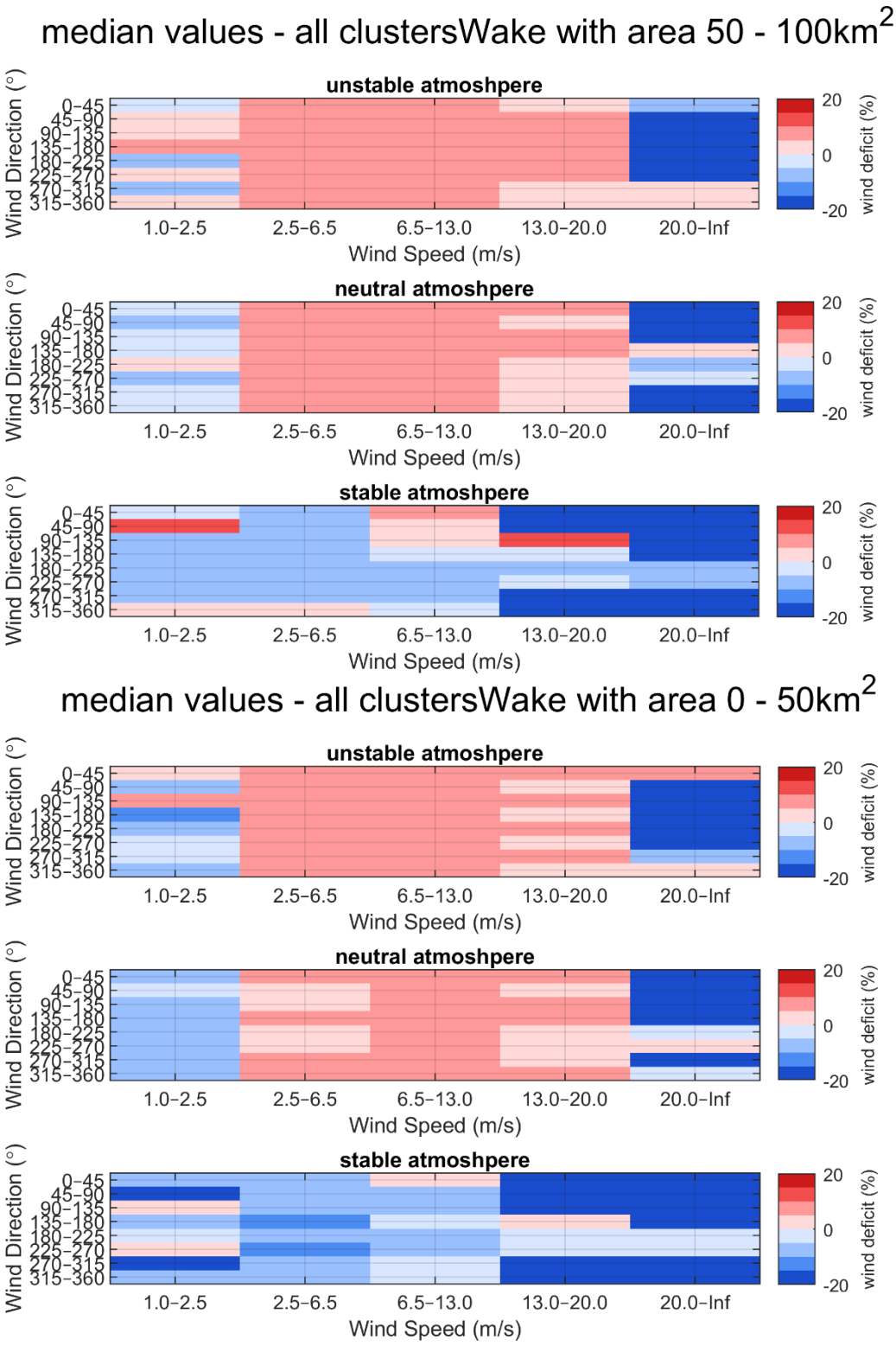
median values - all clustersWake with area 50 - 100km2
unstable atmoshpere
neutral atmoshpere
stable atmoshpere
Wind Direction (°)
0-45
45-90
90-135
135-180
180-225
225-270
270-315
315-360
1.0-2.5
2.5-6.5
6.5-13.0
13.0-20.0
20.0-Inf
Wind Speed (m/s)
wind deficit (%)
20
0
-20
median values - all clustersWake with area 0 - 50km2
unstable atmoshpere
neutral atmoshpere
stable atmoshpere

B Full results: dependencies of current velocity difference due to OWFs operation

B.1 Dependency on wind speed

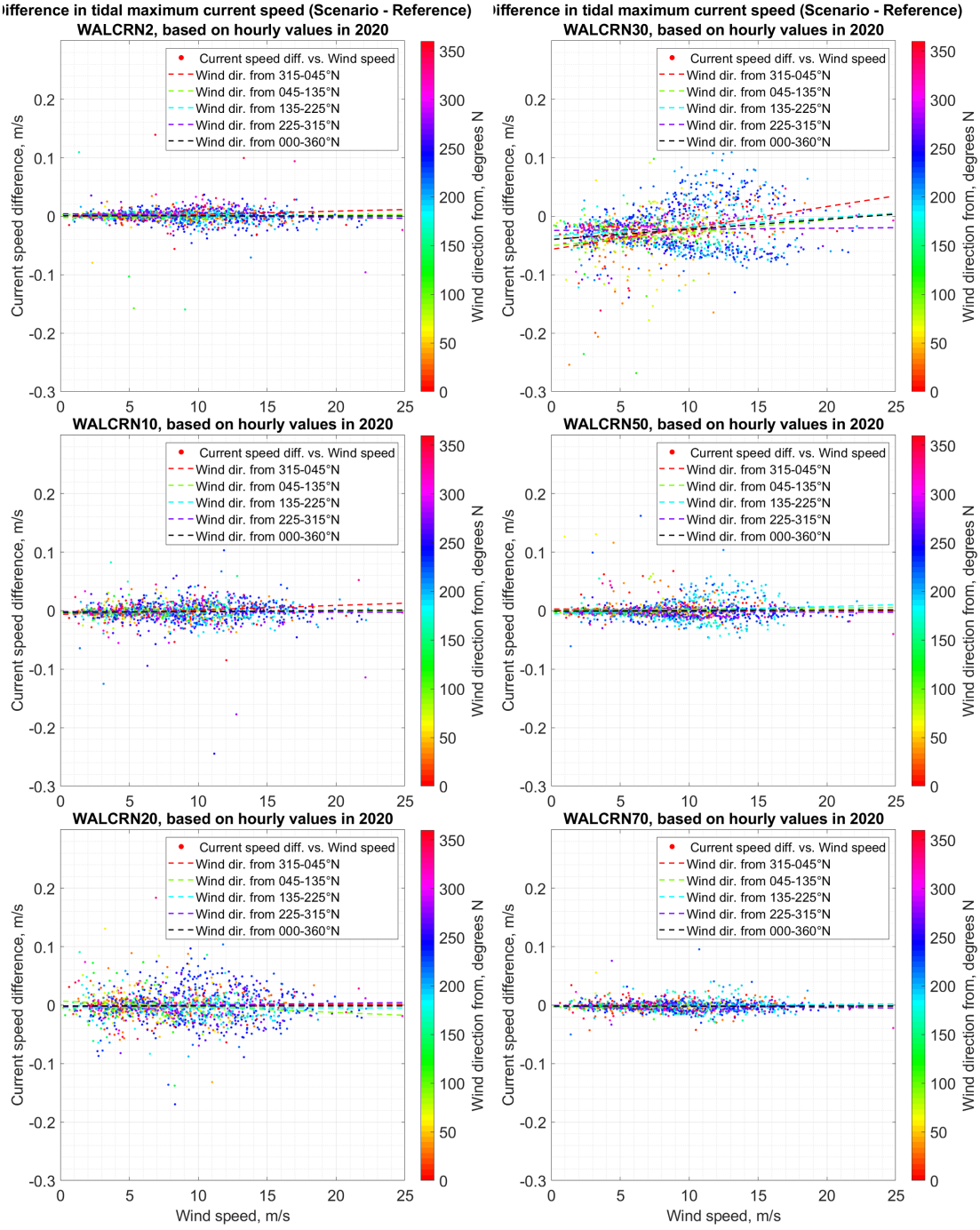

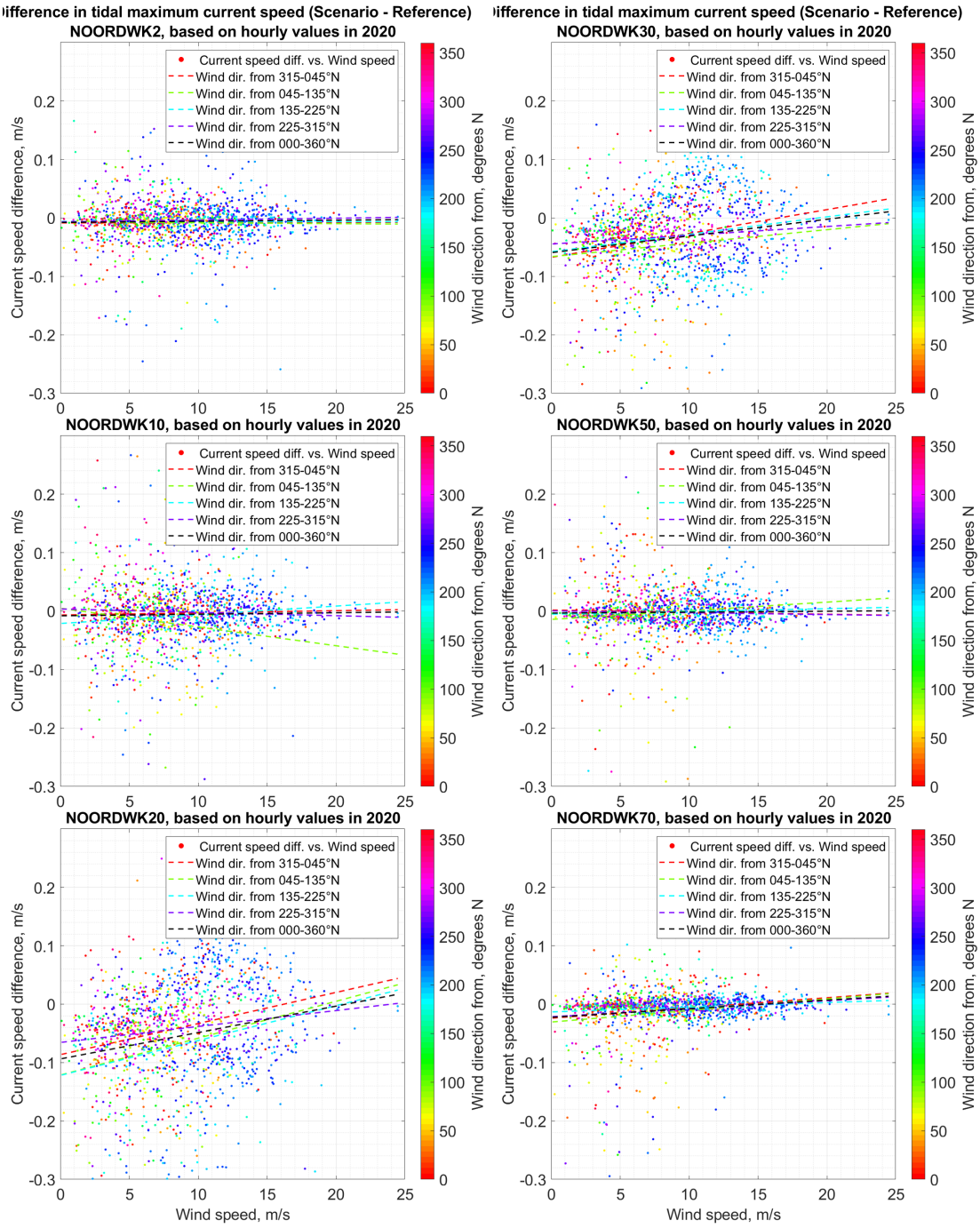
Difference in tidal maximum current speed (Scenario - Reference)
NOORDWK2, based on hourly values in 2020
NOORDWK30, based on hourly values in 2020
NOORDWK10, based on hourly values in 2020
NOORDWK50, based on hourly values in 2020
NOORDWK20, based on hourly values in 2020
NOORDWK70, based on hourly values in 2020
Current speed diff. vs. Wind speed
Wind dir. from 315-045°N
Wind dir. from 045-135°N
Wind dir. from 135-225°N
Wind dir. from 225-315°N
Wind dir. from 000-360°N
Current speed difference, m/s
Wind direction from, degrees N
Wind speed, m/s

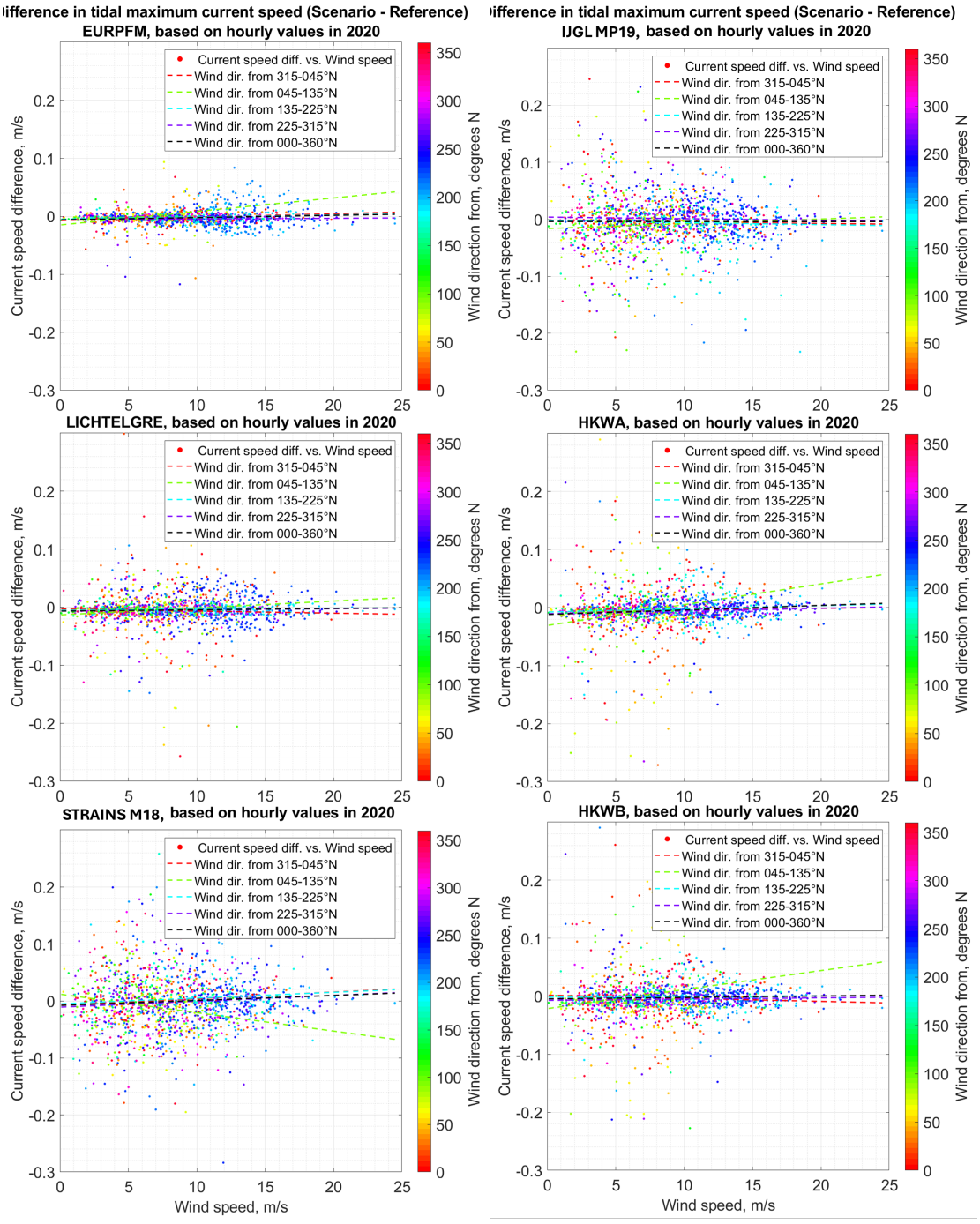
Difference in tidal maximum current speed (Scenario - Reference)
EURPFM, based on hourly values in 2020
Difference in tidal maximum current speed (Scenario - Reference)
IJGL MP19, based on hourly values in 2020
LICHTELGRE, based on hourly values in 2020
HKWA, based on hourly values in 2020
STRAINS M18, based on hourly values in 2020
HKWB, based on hourly values in 2020
Current speed diff. vs. Wind speed
Wind dir. from 315-045°N
Wind dir. from 045-135°N
Wind dir. from 135-225°N
Wind dir. from 225-315°N
Wind dir. from 000-360°N
Current speed difference, m/s
Wind direction from, degrees N
Wind speed, m/s

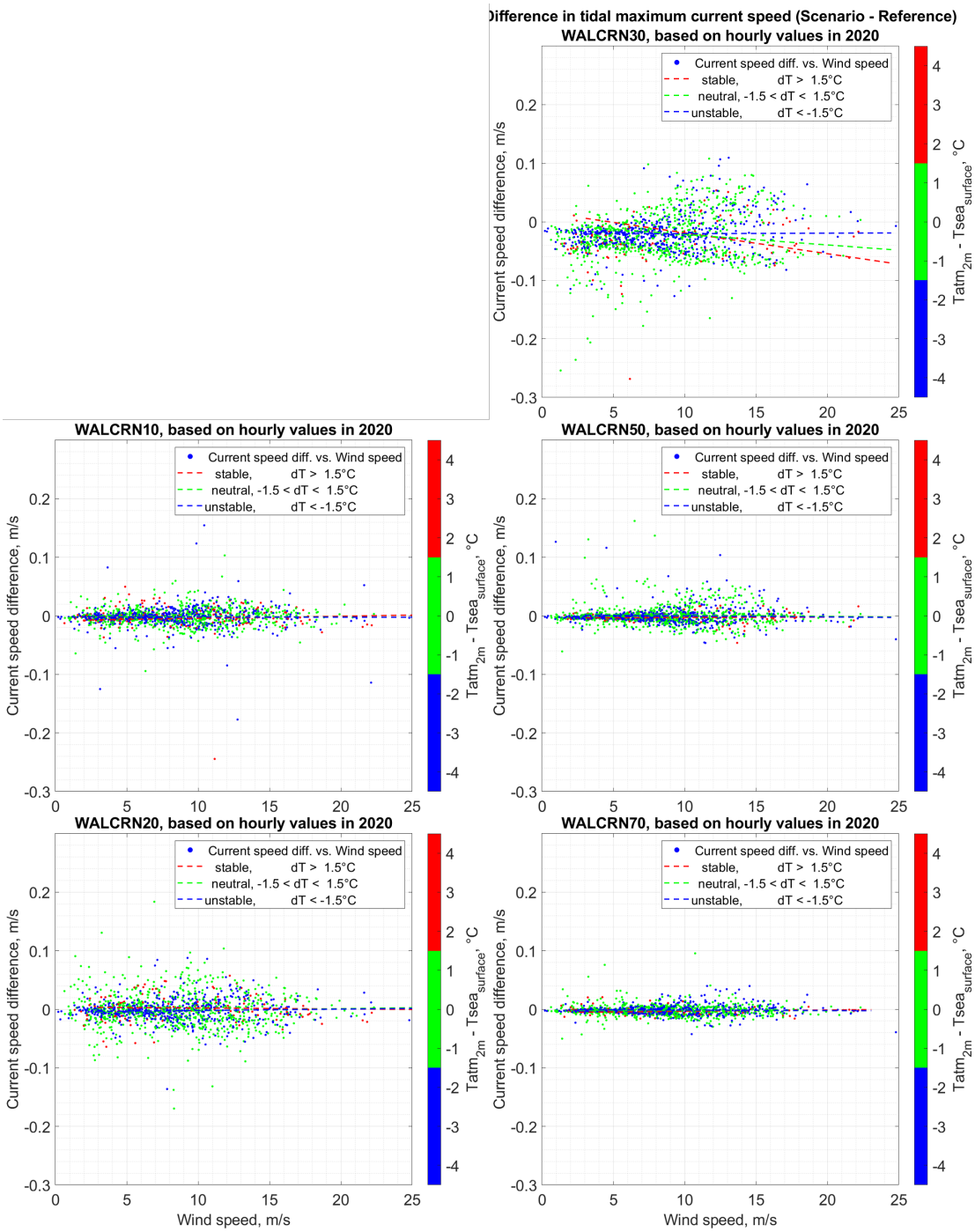
Difference in tidal maximum current speed (Scenario - Reference)
WALCRN30, based on hourly values in 2020
WALCRN10, based on hourly values in 2020
WALCRN50, based on hourly values in 2020
WALCRN20, based on hourly values in 2020
WALCRN70, based on hourly values in 2020
Current speed diff. vs. Wind speed
stable, dT > 1.5°C
neutral, -1.5 < dT < 1.5°C
unstable, dT < -1.5°C
Current speed difference, m/s
Wind speed, m/s
Tatm2m - Tsea surface, °C

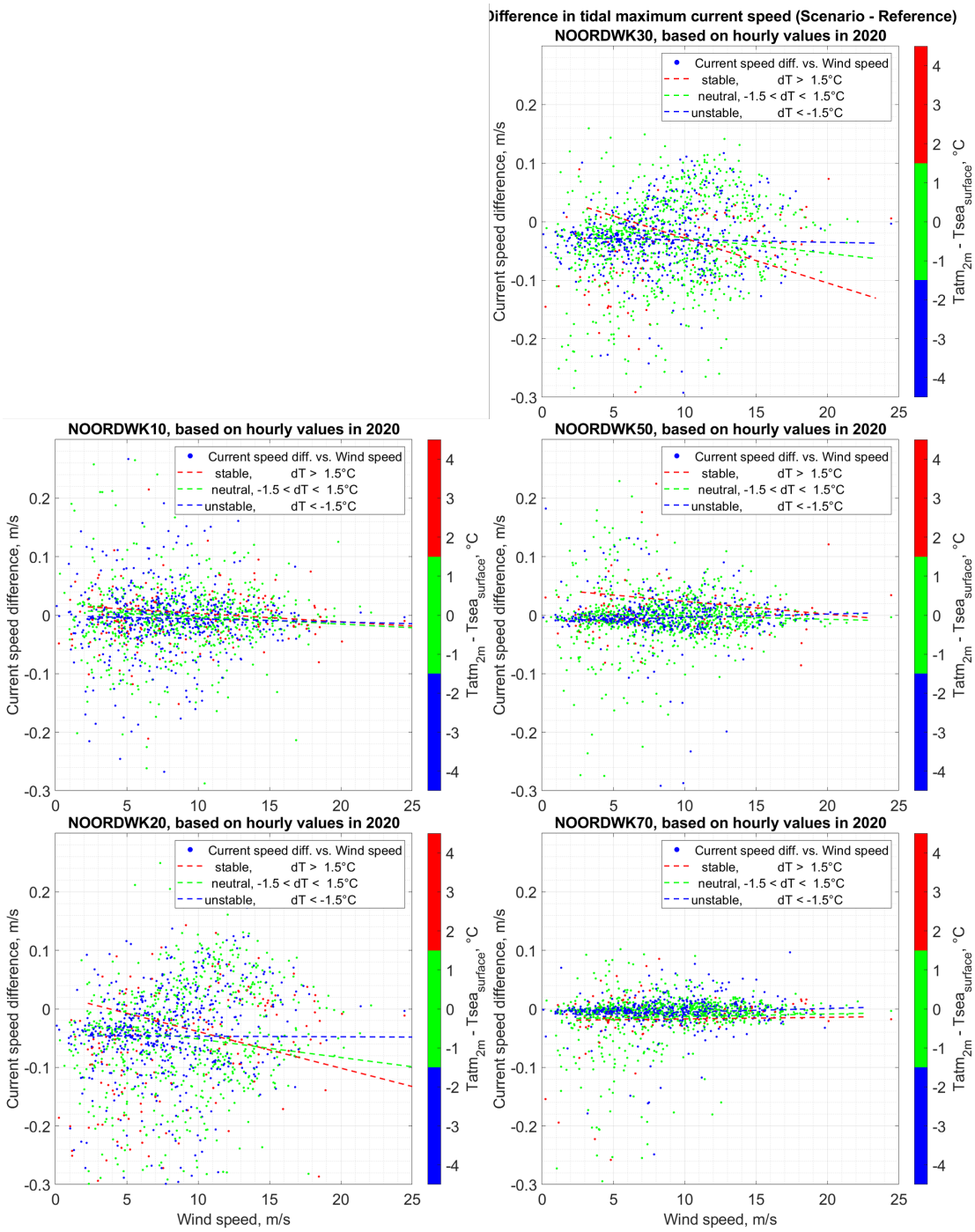
Difference in tidal maximum current speed (Scenario - Reference)
NOORDWK30, based on hourly values in 2020
NOORDWK10, based on hourly values in 2020
NOORDWK50, based on hourly values in 2020
NOORDWK20, based on hourly values in 2020
NOORDWK70, based on hourly values in 2020
Current speed diff. vs. Wind speed
stable, dT > 1.5°C
neutral, -1.5 < dT < 1.5°C
unstable, dT < -1.5°C
Current speed difference, m/s
Wind speed, m/s
Tatm2m - Tseasurface, °C

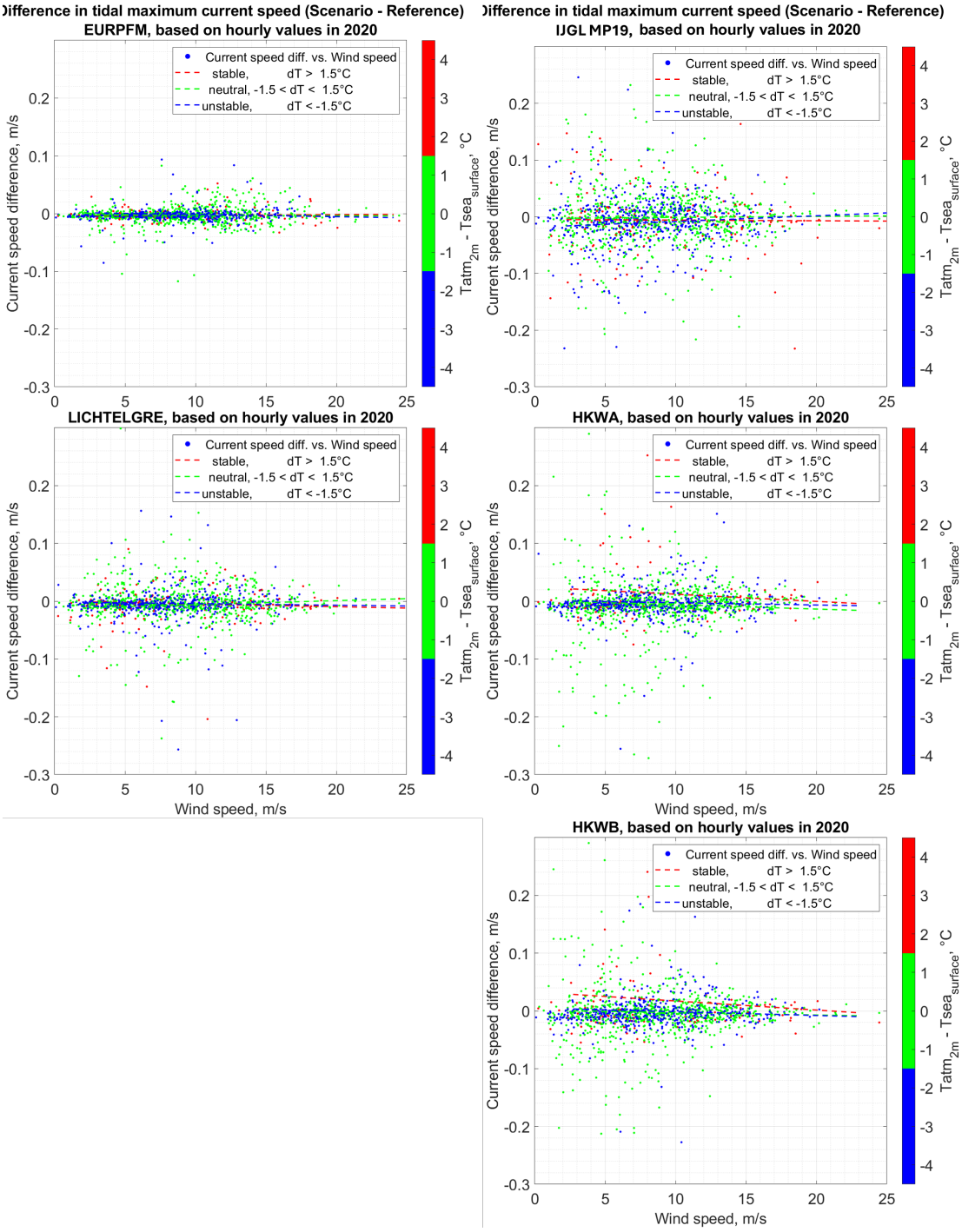
Difference in tidal maximum current speed (Scenario - Reference)
EURPFM, based on hourly values in 2020
Difference in tidal maximum current speed (Scenario - Reference)
IJGL MP19, based on hourly values in 2020
LICHTELGRE, based on hourly values in 2020
HKWA, based on hourly values in 2020
HKWB, based on hourly values in 2020
Current speed diff. vs. Wind speed
stable, dT > 1.5°C
neutral, -1.5 < dT < 1.5°C
unstable, dT < -1.5°C
Current speed difference, m/s
Wind speed, m/s
Tatm2m - Tseasurface, °C

B.2 Dependency on wind direction

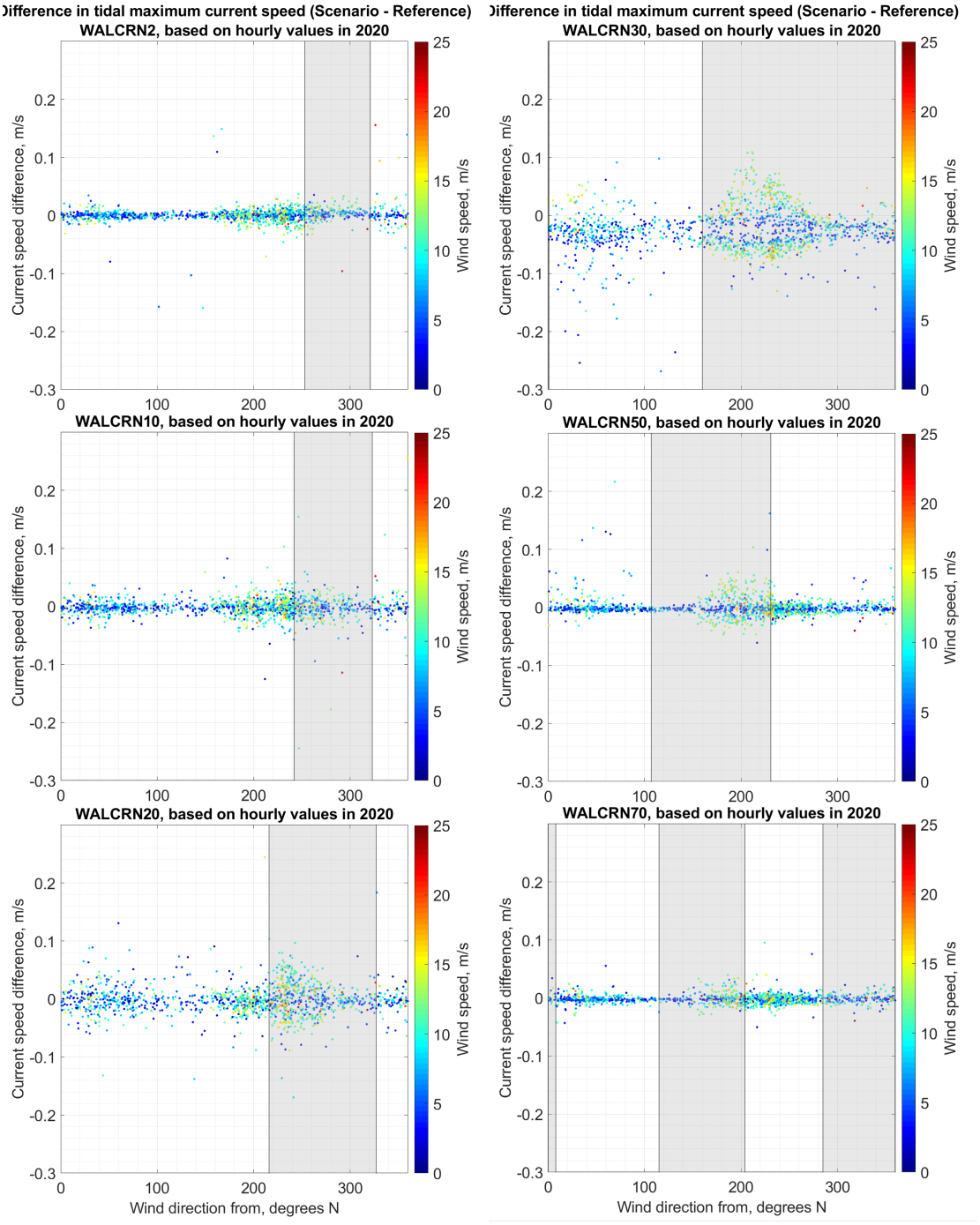

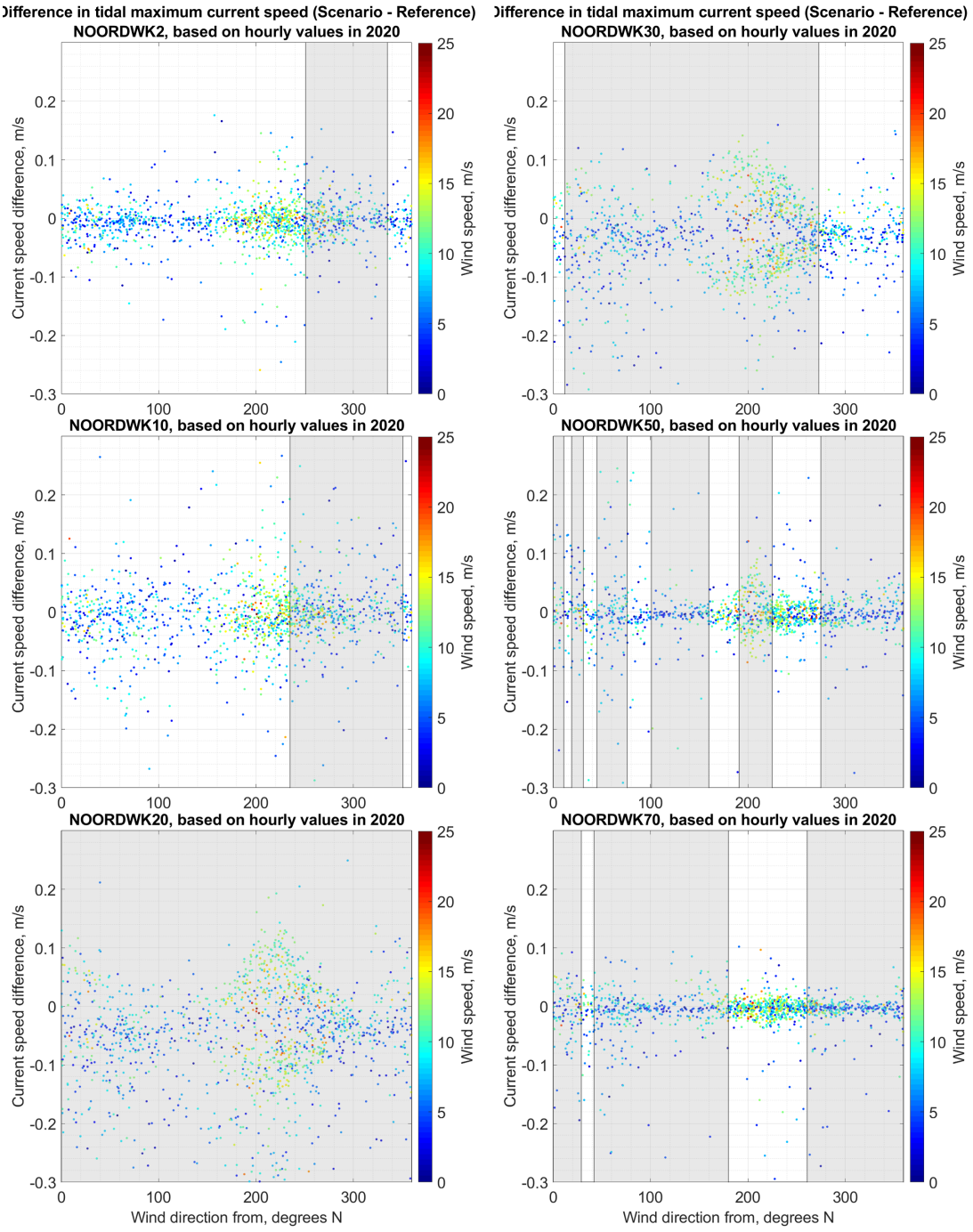
Difference in tidal maximum current speed (Scenario - Reference)
NOORDWK2, based on hourly values in 2020
Difference in tidal maximum current speed (Scenario - Reference)
NOORDWK30, based on hourly values in 2020
NOORDWK10, based on hourly values in 2020
NOORDWK50, based on hourly values in 2020
NOORDWK20, based on hourly values in 2020
NOORDWK70, based on hourly values in 2020
Current speed difference, m/s
Wind speed, m/s
Wind direction from, degrees N

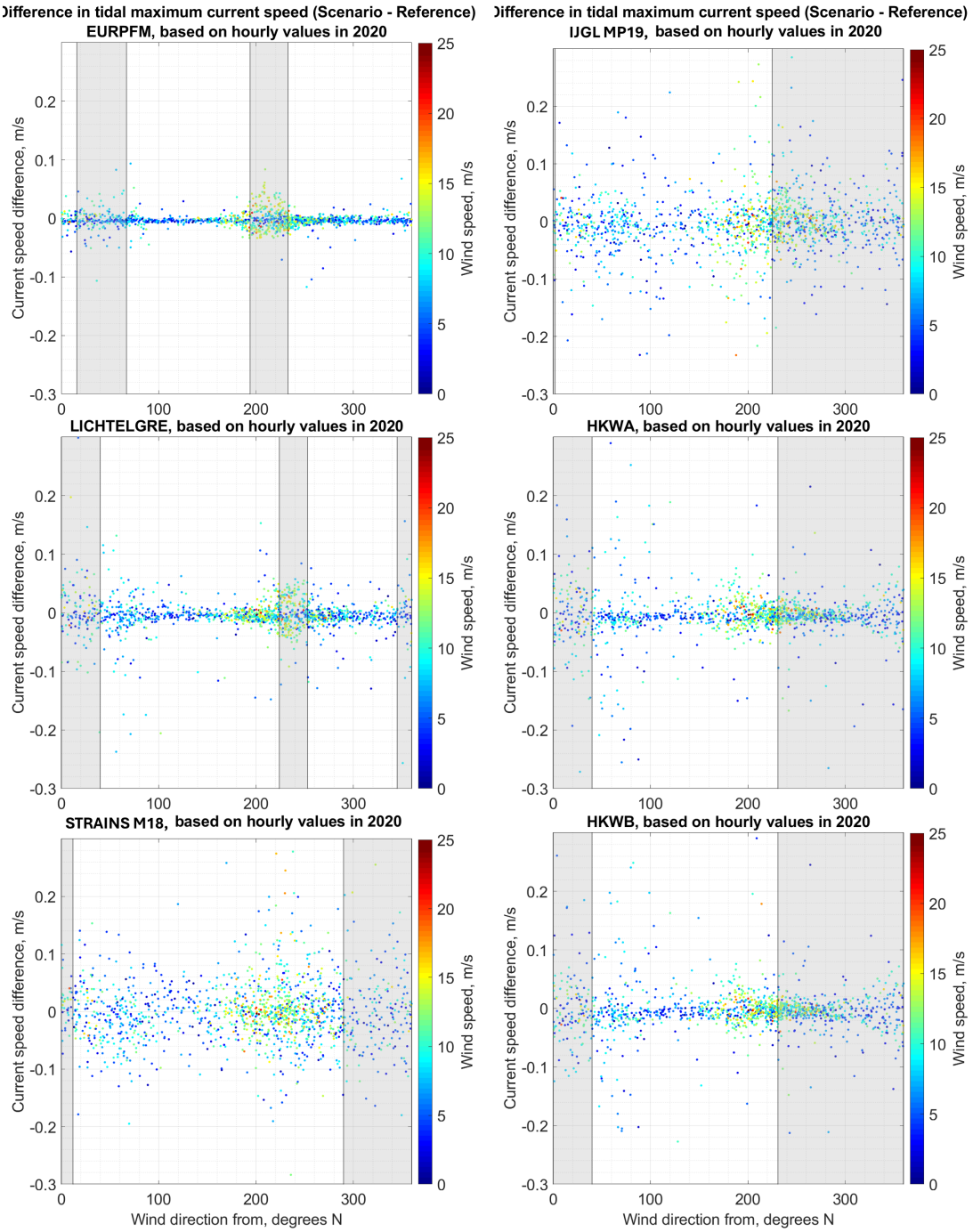
Difference in tidal maximum current speed (Scenario - Reference)
EURPFM, based on hourly values in 2020
Difference in tidal maximum current speed (Scenario - Reference)
IJGL MP19, based on hourly values in 2020
LICHTELGRE, based on hourly values in 2020
HKWA, based on hourly values in 2020
STRAINS M18, based on hourly values in 2020
HKWB, based on hourly values in 2020
Current speed difference, m/s
Wind speed, m/s
Wind direction from, degrees N

Deltares is an independent institute for applied research in the field of water and subsurface. Throughout the world, we work on smart solutions for people, environment and society.

Deltares

www.deltares.nl